UNIVERSITÀ DEGLI STUDI DI MILANO

PhD Course

Integrated Biomedical Research

Cycle XXIX

BIO-09

Embryonic stem cell-derived sinoatrial-like cells as a model to study the exercise-dependent effects of miR-1 and miR-423 upregulation on heart rate

Dr. Angelica Gualdoni

Tutor: Prof. Andrea Francesco Barbuti

Coordinatore: Prof.ssa Chiarella Sforza

Summary

1. Abstract

The cardiovascular benefits of regular exercise are well established. High-intensity endurance exercise induces electrical, structural, and functional adaptations in the heart in order to sustain the increased cardiac output and metabolic needs. These cardiac changes are called 'athletes heart' and include typical morphological changes (eccentric hypertrophy) and a slowing of the heart rate with significant brady- and tachy-arrythmias. The heart rhythm depends on the intrinsic heart rate, generated by the pacemaker cells in the sinus node, and on the autonomic (parasympathetic and sympathetic) tone. Bradycardia in endurance athletes is commonly attributed to an increased vagal tone. Recently, D'Souza and colleagues have instead demonstrated that, in rodent, training-induced bradycardia is due to an intrinsic modification of the heart. In particular, they showed that bradycardia persists (*in vivo*) after blockade of the autonomous nervous system in mice and (*in vitro*) in the isolated heart. Furthermore, they demonstrated a reduction of the I_f pacemaker current in sinoatrial node (SAN) cells of trained mice. The molecular mechanism at the basis of this process is not completely understood but our collaborators in Manchester showed also a training-dependent up-regulation of miR-1, one of the main myomiR, and of miR-423.

The aim of this work is to understand the role of miR-1 and miR-423 in sinoatrial cells. Given the difficulty to keep SAN cells in culture, we decided to study the role of these microRNAs in sinoatrial-like cells differentiated from mESC overexpressing them. To do this, we generated three different clones of mouse embryonic stem cells overexpressing miR-1, miR-423 and a control line. The overexpression of these miRNAs affected neither the pluripotency nor the capacity of mESC to differentiate into cardiomyocytes. We selected CD166+ sinoatrial-like cells from differentiating mESC by flow cytometry and found that the proportion of CD166+ SAN-like cells is higher in mESC-miR1 (25.20±2.32% n=26) and in mESC-miR423 (18.56±1.36% n=9) than in control lines (11.09±1.09% n=30).

Electrophysiological analysis showed a lower firing rate in miR-1-CD166+ cells than in cells from the control line, while no differences are present between miR-423-CD166+ and empty-CD166+ (miR-1-CD166+ 1.37±0.08Hz n=10; miR-423-CD166+

2.36±0.30Hz n=7; empty-CD166+ 2.22±0.22Hz n=7). We further demonstrated that the miR-1 overexpression leads to around a 50% reduction of the funny current.

We found no differences in the expression level of miR-423 in miR-423-CD166+ and empty-CD166+, despite it resulted overexpressed in mESC-miR-423 respect to mESC-empty. We then studied the effect of miR-423 by transiently overexpressing it in neonatal rat ventricular cardiomyocytes, finding again no differences.

These data demonstrated that miR-1 modulates the beating frequency of sinoatrial-like cells, reducing the I_f current, and thus demonstrating that miR-1 contribute to the establishment of the endurance athletes' bradycardia. For what concern miR-423, from our data it seems to have no effect in the control of cardiac rate, however, since the overexpression of miR-423 was modest in mESC and we could not control the expression level in transfected neonatal rat ventricular cardiomyocytes further experiments are needed to definitely rule out its contribution to exercise-induced bradycardia.

2. Introduction

2.1 The Heart

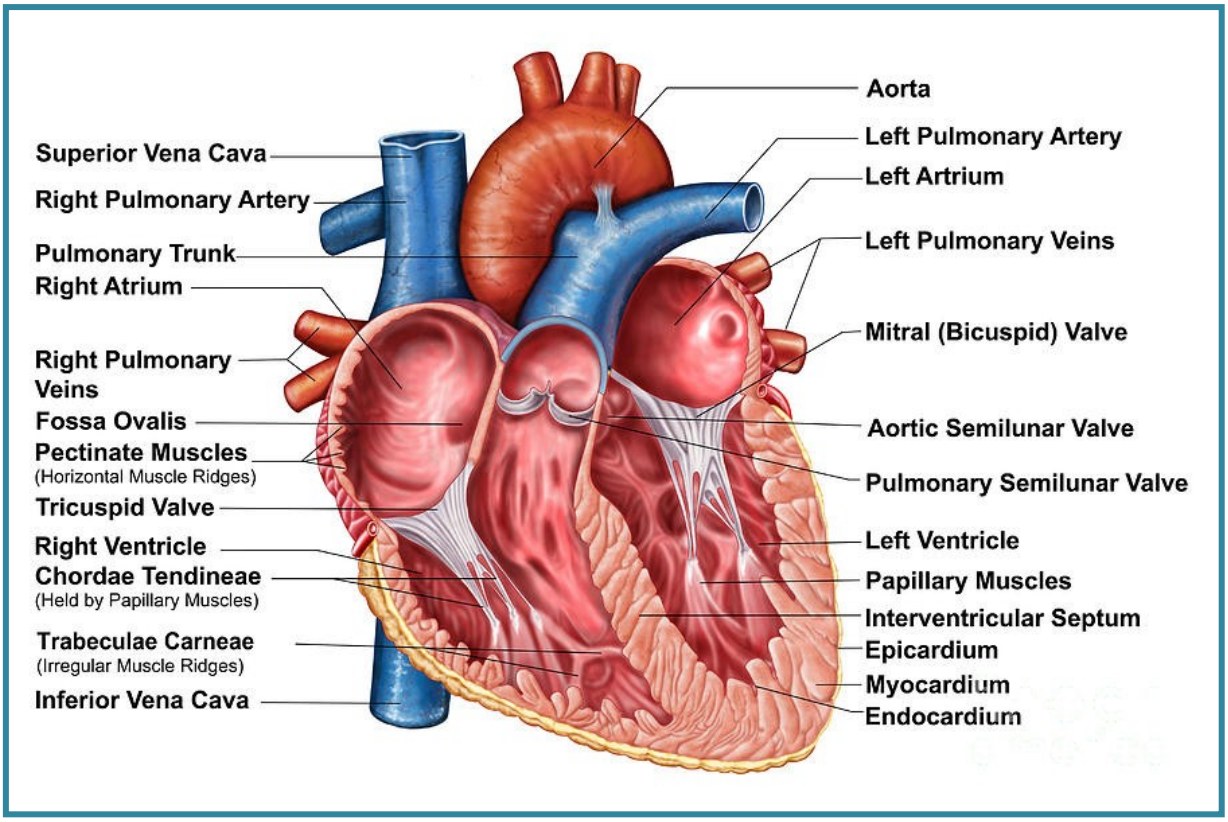

Fig. 1: anatomy of the heart, frontal section.

The heart is a hollow and muscular organ, it acts as a mechanical pump allowing blood circulation into the body. It is composed by four cavities, divided by a septum into two non-communicating sectors, the right and left heart. Each sector is composed of an atrium (upper chamber) and a ventricle (lower chamber). Atria and ventricles are connected by the atrioventricular (AV) valves that allows the blood to flow only from the atria to the ventricles. The AV valve on the right side of the heart is called tricuspid, while the valve on the left side is termed mitral or bicuspid. Atria are smaller and have thinner muscular walls than ventricles. Ventricles, on the other hand, have thicker myocardial walls, with the left much thicker than the right, because it has to pump blood throughout the high resistance systemic circulation. The right atrium receives the blood low in oxygen from the superior and inferior vena cava and sends it to the right ventricle, which sends out the blood through the pulmonary valves to the pulmonary artery and to the lungs; here the blood is

oxygenated and comes back to the heart from the pulmonary veins to the left atrium, after that it goes into the left ventricle and to all body through the aortic valves and the aorta. The pulmonary and the aortic valves are the semilunar valves and they prevent the return of blood from arteries to ventricles.

The heart is located into the chest, in the lower anterior mediastinum and leans on the diaphragm. It is located into the pericardium, that is a serous membrane that produces a serous fluid that reduces friction and allows the movements of the heart. The pericardium has one parietal and one visceral layer; the second one is intimately connected to the heart forming the epicardium, the outer of the three layers of the heart wall. The other two are the endocardium, a squamous endothelium that covers the interior surface of the heart, and the myocardium, the muscular middle layer that makes up the majority of the thickness and mass of the heart.

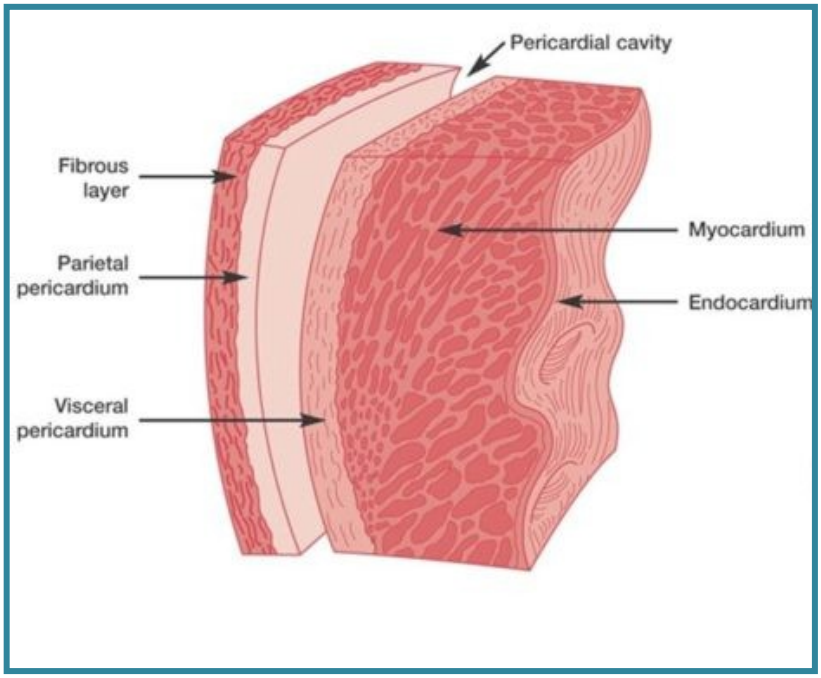

Fig. 2: layers of the heart.

The heart is composed of different types of muscle cells, which are commonly classified into contractile myocardium and conduction system. The contractile cells are the cells of the working myocardium connected through low-resistant gap junctions; in this way every cell of the heart is electrically coupled to the next one and the heart can be considered a functional syncytium. The working myocardium represents the major portion of atria and ventricles. Instead, cells of the conduction system are specialized cells involved in the generation and propagation of the action

potentials to allow the spontaneous contraction of the heart. The conduction system is composed of the sinoatrial node (SAN), the atrioventricular node (AVN), the bundle of His, and the Purkinje fibers. The SAN is located into the right atrium near the entrance of the superior vena cava and generates spontaneous action potentials. This action potentials propagate to the rest of the heart and thus the SAN is the pacemaker region. The action potentials will first be propagated to the atria that are the first structures to contract and from there, the signal reaches the AVN, located in the right posterior portion of the interatrial septum. The AVN has two main functions: conducting the depolarization from atria to ventricles, indeed AVN is normally the only conductive link between the two chambers, and delaying the spread of excitation, allowing the consecutive contraction of atria and ventricles. The AVN is in connection with the bundle of His that divides first into two branches and then into the Purkinje fibers, an extensive network of fibers that conducts action potential very rapidly throughout the ventricles.

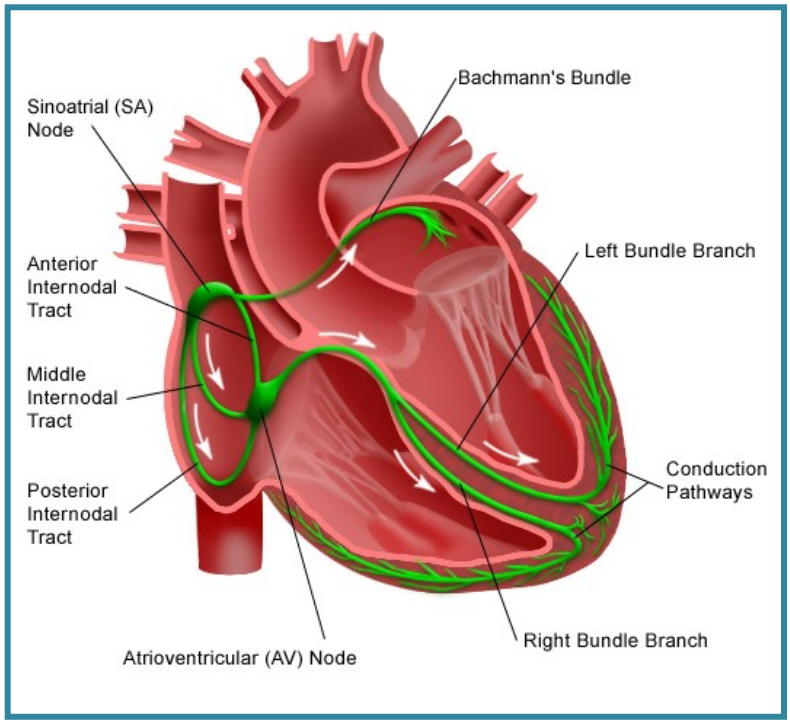

Fig. 3: conducting system of the heart.

All the components of the conduction system are able to spontaneously generate action potentials, but the SAN does it at a higher rate, concealing the activity of the other portions through a mechanism known as “overdrive suppression”.

The heart is innervated by the autonomic nervous system, which is divided into the sympathetic and parasympathetic branches. Sympathetic stimulation of the heart induces an increment of heart rate, force of muscular contraction, and of conduction velocity and it acts releasing norepinephrine that binds to β-receptors. Parasympathetic stimulation has the opposite effects, which are mediated by acetylcholine that binds to muscarinic receptors. Under resting condition, both autonomic divisions send stimuli to the heart, and especially to the SAN, but normally in humans the dominant influence is parasympathetic. Thus, although the heart beats spontaneously, it exhibits a vagal tone and the heart rate is usually lower than the intrinsic rate.

2.2 The action potential

The action potential represents the changes in voltage of a single cardiac cell. Different action potentials could be recorded in different regions of the heart. There are two primary types of action potentials: atria and ventricles have fast-response action potentials, while SAN and AVN cells display a slow-response action potentials. Fast-response action potentials could be subdivided into five phases (Fig. 4):

- Phase 0 (fast depolarization): this phase is characterized by a rapid upstroke due to a fast Na^+ current (I_{Na}). The sodium channels have an opening threshold around -70mV, while the cells have a resting potential of -90mV, so it is necessary a depolarizing stimulus in order to start the action potential that comes from the depolarization of the adjacent cell.
- Phase 1: it represents a small and transient repolarization caused by the opening of a special type of transient outward K+ channel (I_{to}).
- Phase 2: it is the plateau phase of the action potential. This plateau phase is due to the balance of inward calcium currents generated by calcium channels (I_{CaL} and I_{CaT}) and outward potassium currents (I_{Kr}, I_{Ks}) that maintains the membrane potential near 0mV for about 200ms, prolonging the action potential duration and permitting the excitation-contraction coupling.
- Phase 3: during this phase the membrane potential repolarizes to the resting value, thanks to the inactivation of calcium channels and the active presence of potassium channels; the potassium currents responsible for this phase are the rapid (I_{Kr}) and slow (I_{Ks}) component of the delayed outward currents.

- Phase 4: the membrane potential is maintained at the resting value of about -90mV by the inward rectifier current (I_{K1}) until the incoming of a new depolarizing stimulus.

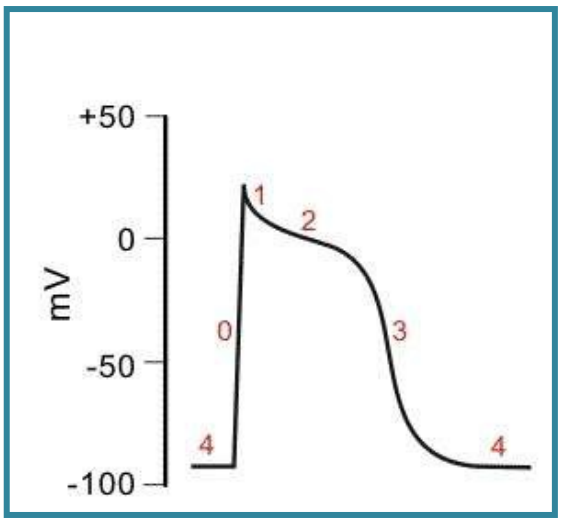

Fig. 4: schematic representation of fast response action potential.

Slow-response action potential:

The main characteristic of the SAN cells is the ability to generate regular and spontaneous action potentials, known as “slow response” action potential (Fig. 5). The main characteristic of the slow response action potential is the absence of both a true resting potential and a plateau phase. It is characterized by the following phases:

- Phase 4: early diastolic depolarization (EDD). In these cells, there is not a resting potential, and the most negative potential that the cells reach between two APs is called Maximum Diastolic Potential (MDP). This phase is characterized by the activation of a slow, inward, depolarizing current, called “funny” current (I_f) (*DiFrancesco, 1986 b*). This current leads to a depolarization of the membrane potential. It is also present a spontaneous calcium release from the sarcoplasmic reticulum that contributes to the late phase of the diastolic depolarization by activating the Na^+/Ca^{++} exchanger (*Lakatta & DiFrancesco, 2009*). The EDD phase of slow-response action potential is also characterized by the absence of I_{k1}.
- Phase 0: this phase is characterized by a depolarizing calcium current mediated by both Transient (T-type) and Long-lasting (L-type) calcium channels. The T-type calcium channels have a threshold of -60mV, while the L-type starts to activate at more positive potential (around -40 mV).

Therefore in the slow response action potential the up-stroke phase is not due to a sodium current, but to a calcium current, so the steepned of this phase is lower in SAN than in ventricles.

- Phase 3: this phase is characterized by the inactivation of calcium channels and by the opening of potassium channels (*Mangoni and Nargeot 2008*).

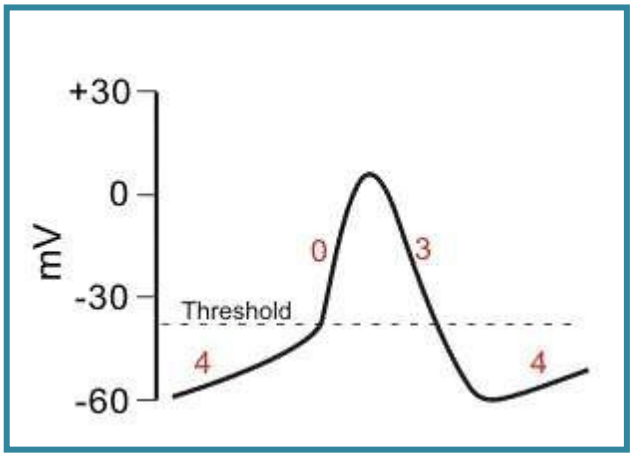

Fig. 5: schematic representation of slow response action potential.

2.3 The I_f current and the HCN channels

The funny current (I_f, pacemaker current) was first described in the SAN (*Brown et al., 1979*) and was extensively characterized originally in this tissue and in Purkinje fibers (*DiFrancesco et al., 1986 a; DiFrancesco, 1986 b; Brown et al., 1980; DiFrancesco et al., 1980; DiFrancesco, 1981 a; DiFrancesco, 1981 b*). This current has peculiar characteristics: it is a mixed current of sodium and potassium and it is activated by both membrane hyperpolarization, with a threshold of approximately -30/-40mV, and cyclic nucleotides.

The molecular component of the pacemaker current is the Hyperpolarization-activated Cyclic Nucleotide-gated channel (HCN), that is a family composed of 4 members (HCN1, HCN2, HCN3, and HCN4), belonging to the superfamily of voltage-gated K^+ (Kv) and CNG channels; they have a tetrameric composition (*Ulens & Siegelbaum, 2003; Zagotta et al., 2003*), and each subunit is composed of 6 transmembrane domains (S1–6); the segment S4 is the voltage sensor. The pore of the HCN channels is composed of the GYG sequence, typical of potassium

channels, and the C-terminus contains the CNBD, the cyclic nucleotide-binding domain, that confers sensitivity to cyclic nucleotides (*Viscomi et al., 2001*). Direct binding of cAMP molecules to the C-terminus of pacemaker channels increases the opening probability of HCN channels via a positively-directed shift of the voltage dependence of the activation curve, whereas a reduced intracellular cAMP concentration gives rise to the opposite action (*DiFrancesco & Tortora, 1991*). The intracellular concentration of cAMP is modulated by the binding of sympathetic and parasympathetic neurotransmitters to β-adrenergic and muscarinic receptor, respectively; consequently, the I_f current is modulated by the autonomic nervous system. As previously described, the I_f current is involved in the EDD phase of action potential, so an increase or a decrease of the net current leads to a change in the slope of EDD and therefore to an increase or decrease of the firing rate (*DiFrancesco e Borer, 2007*). Pacemaker channels, and specifically HCN4 isoform, are confined, together with the β2-adrenergic receptors (β2-ARs), to membrane *caveolae*, cellular microdomains whose function is to keep in close proximity proteins involved in a specific signal transduction pathway (*Barbuti et al., 2007*).

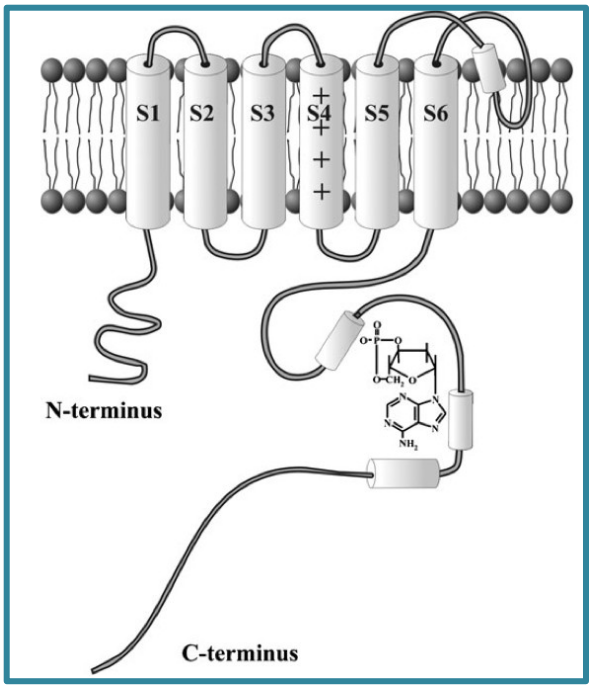

Fig. 6. HCN channels structure.

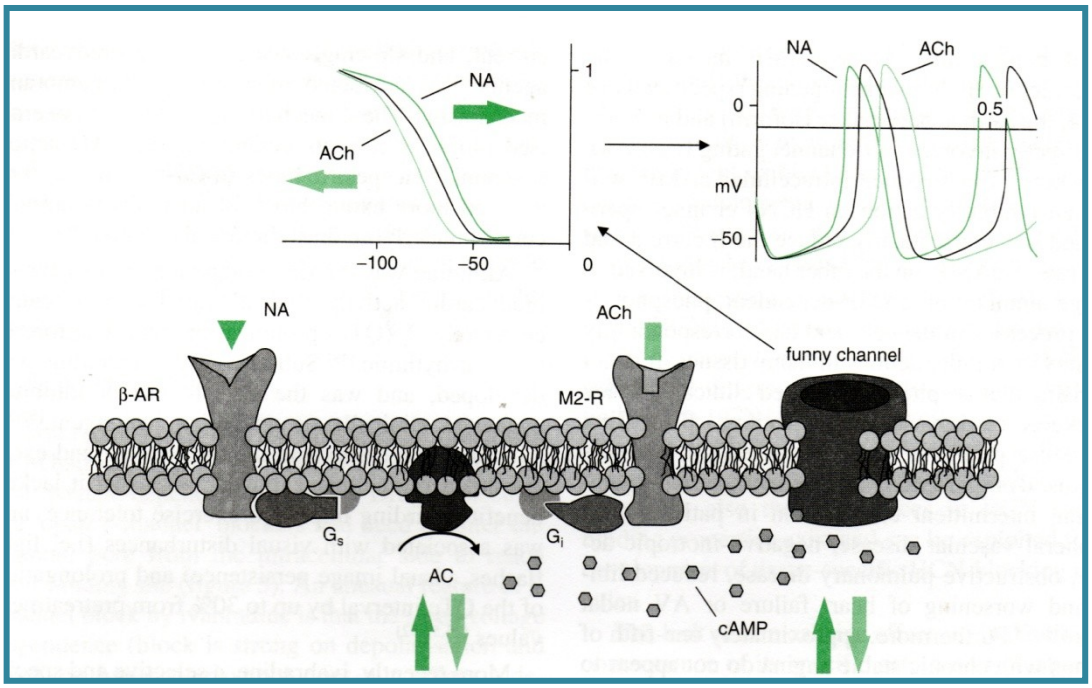

Fig. 7. schematic representation of HCN cannels regulation by autonomic nervous system. ACh = acetylcholin, AC = adenylate cyclase, β-AR = β-adrenergic receptor, Gi = inhibitory G protein, Gs = stimulatory G protein, M2-R = Muscarinic receptor type-2, NA = noradrenalin (*DiFrancesco e Borer, 2007*).

The I_f pacemaker current is predominantly, but not exclusively, expressed in the conduction system of the heart, indeed it is present also in the working myocardium but at much lower level and its physiological role is not completely clear. However, it seems to be involved in pathologic conditions, for example, I_f is upregulated in ventricular myocytes of hypertrophic hearts as a consequence of remodeling, leading to the hypothesis that it may contribute to arrhythmias in chronic hypertension and cardiac failure, a condition associated with increased risk for sudden cardiac death (*Cerbai et al., 2006*). Moreover, the HCN channels are differently distributed in different heart regions, in particular HCN4 is the main isoform of SAN cells despite HCN1 and 2 being expressed at lower level. HCN2 is expresses at very low level in ventricles and atria (*Shi et al., 1999; Brioschi et al., 2009)*. The different HCN channel isoforms have some common characteristics, in particular, the transmembrane segments, the core region and the CNBD are extremely conserved but they have differences at N- and C- terminus, in the activation and deactivation kinetics and in the affinity to cyclic nucleotides (*Viscomi et al., 2001; Altomare et al., 2001; Zagotta et al., 2003*).

2.4 SAN development

The heart derives from the embryonic mesoderm, organized in the “primitive heart tube” that after the cardiac looping further develops forming the cardiac chambers (*Moorman e Christoffels, 2003*). The SAN precursors develop from the region of the sinus venosus, which separates from the rest of cardiac mesoderm at day 8 (E8) of differentiation. At E8.5 these precursors are characterized by the specific expression of a series of transcription factors such as Tbx18, Isl-1 while do not express Nkx2.5, a transcription factor that, together with Tbx5, is responsible for the specification of the working myocardium (*Mommersteeg et al., 2010*). At E9.5 Tbx3 and Shox2 start to be expressed in those precursors that will form the conduction system; Tbx3 is a transcription factor that specifically inhibits the expression of Nppa and Cx40, characteristic of atrial tissue, Shox2 is instead essential for the inhibition of Nkx2.5 (*Hoogaars et al., 2004; Espinoza-lewis et al., 2009*). Another fundamental transcription factor for the correct development of the SAN is Pitx2c, indeed, while the sinus venosus is a symmetric structure, the SAN originates only in the right atrium and Pitx2c specifically suppresses the SAN gene pathway in the left region, allowing the correct asymmetric development (*Mommersteeg et al., 2007; Barbuti and Robinson 2015*).

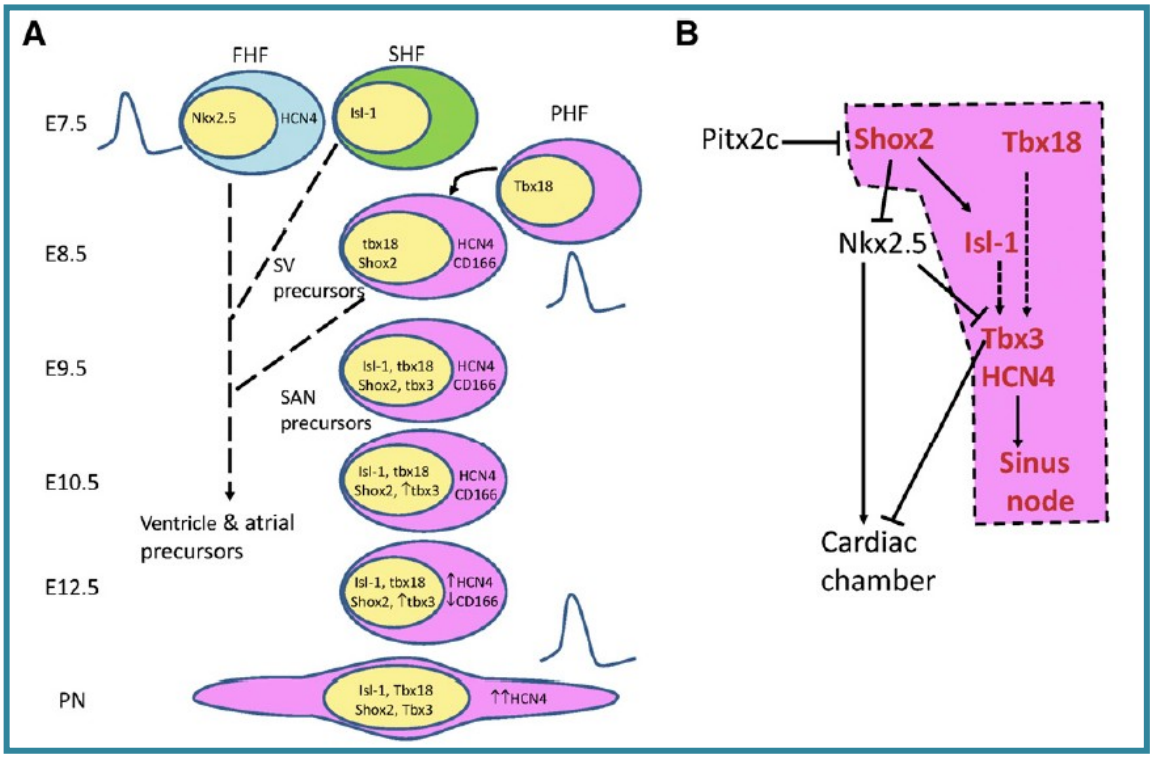

Fig. 8: schematic representation of genes involved in SAN development (from *Barbuti and Robinson 2015*).

2.5 Embryonic stem cells

Embryonic stem cells (ESCs) are pluripotent stem cells derived from the inner cell mass of the blastocyst. ESCs are able to perpetuate themselves *ad infinitum* (self-renewal), and to generate differentiated progeny. ESCs can divide symmetrically and asymmetrically, in the first case they generate two daughter cells with the same fate expanding the pool of stem cells, while in the second situation they originate two cells with different fates: one will maintain the pool of ESC, the other one gives origin to the differentiated progeny. The balance between symmetric and asymmetric division is controlled by environmental signals to produce the right number of stem cells and differentiated daughters (*Morrison et al., 2006*).

ESCs are pluripotent and consequently they are able to differentiate in all cells of the three germ layers.

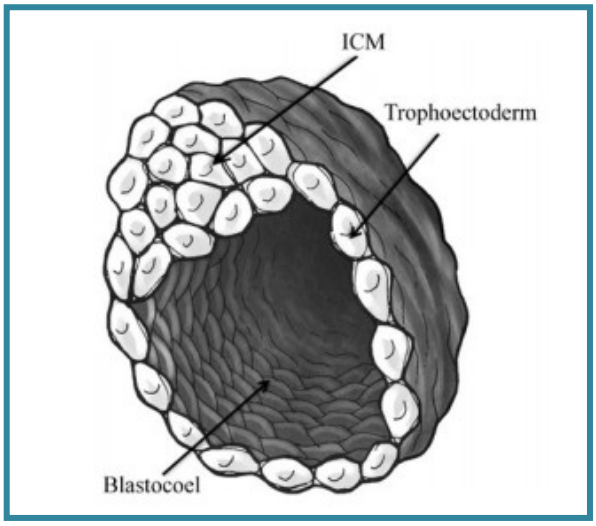

Fig. 9: schematic mammalian embryo at the blastocyst stage. ICM: inner cellular mass (*De Miguel et al., 2010*).

The first mouse embryonic stem cells (mESC) were isolated in the 80s. It is possible to culture mESC *in vitro* for a long time, in the presence of LIF (Leukemia Inhibitory Factor) (*Matsui et al., 1992*). mESCs express specific marker of pluripotency, like glycolipids stage specific embryonic antigen (SSEA-1) or Oct4, Nanog, and Sox2, that are transcription factors that have an essential role in the regulatory circuitry needed to maintain an undifferentiated state and self-renewal (*De Miguel et al., 2010*).

It is possible to induce the differentiation of mESC in all cell types *in vitro*, through the formation of Embryoid Bodies (EBs), macroscopic structures that recapitulate the early stage of embryo development and contains cells of all three germ layers.

2.6 Isolation of sinoatrial-like cells

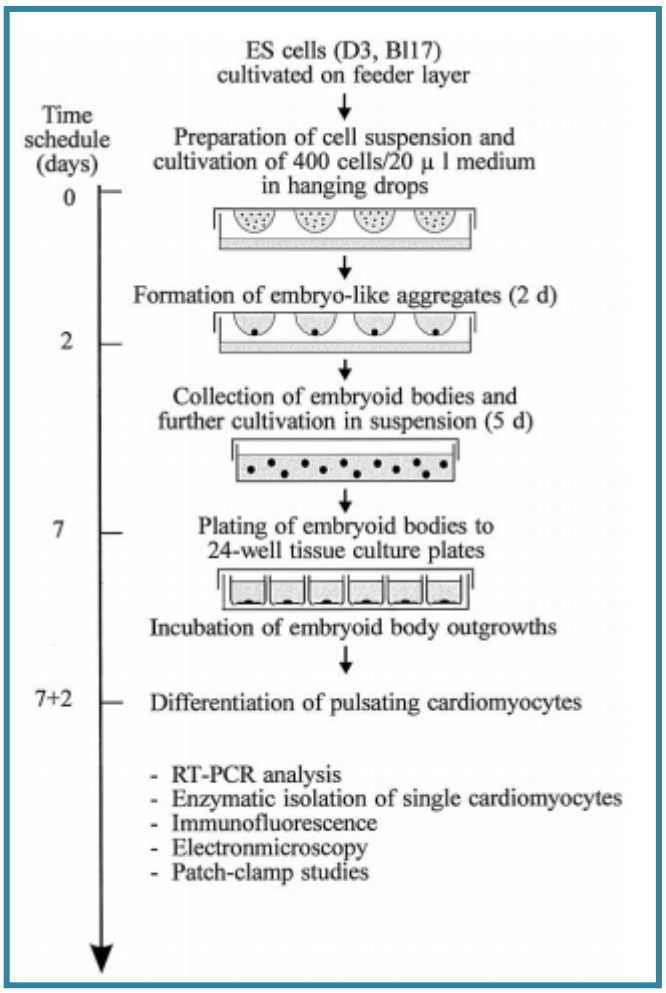

Fig. 10: example of HD technique to EBs differentiation (*Hescheler et al., 1997*)

As previously described, EBs are composed of cells of all three germ layers, and one of the first lineage that appears is the cardiac type. One of the most common and well-defined protocol to obtain beating EBs is based on the hanging drops (HDs) technique. This protocol permits the formation of EBs, that in 80-90% of the cases displays spontaneous beating activity (*Wobus et al., 1991*). It is well known that the cardiomyocytes population into EBs is heterogeneous; atrial-, ventricular-, and sinoatrial-like action potentials could be distinguished (*Maltsev et al., 1993*).

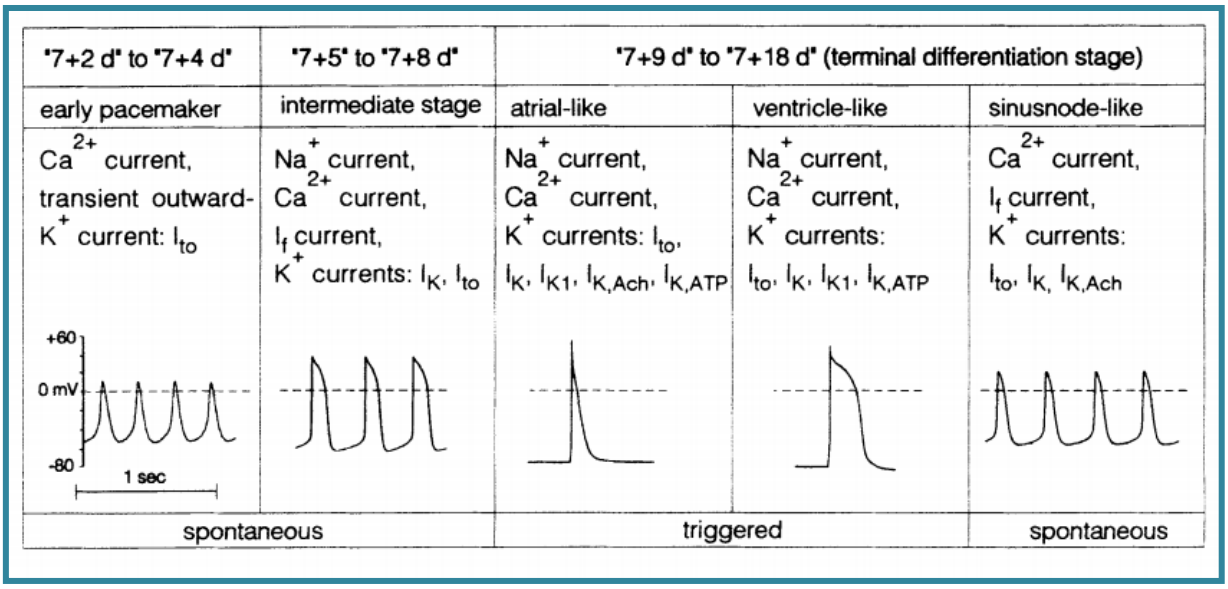

Fig. 11: representative action potentials recorded from cardiomyocytes in EBs (*Maltsev et al., 1994*).

Since the heterogeneity of cells obtained from differentiating mESCs it is necessary to tune a protocol to isolate only cardiac cells, and possibly to discriminate the different cardiac phenotype.

Several approaches were attempted, based on cell-engineering, pharmacology, and analysis of expression markers. Many groups tried to isolate cardiomyocytes from EBs, using a reporter gene: they generated mESCs line expressing a reporter gene, like eGFP, under the control of a promoter of a cardiac gene, like ANP (Atrial Natriuretic Peptide), α-MHC (Alpha-myosin heavy chain), mink, and GATA6. In all these cases, a mixed population of atrial- and sinoatrial-like cells was obtained (*Gassanov et al., 2004; Kolossov et al., 2005; White and Claycomb, 2005*). Hidaka and colleagues isolated a mixed population of ventricular-, atrial-, and sinoatrial-like cells using the eGFP under the control of Nkx2.5, a transcription factor involved in chamber formation (*Hidaka et al., 2003*). The selection based on the activity of HCN4 promoter did not allow to select a pure population of SAN cells, indeed, even though the expression of HCN4 and of the funny current is necessary, it is not sufficient to identify SAN cells, since HCN4 is also expressed by other cell types during embryonic development (*Morikawa et al., 2010; Scavone et al., 2013*).

Different approaches based on the use of drugs were also developed in order to improve cardiac differentiation, without even manipulating the cell genome: treatment with suramin or ET-1 (endothelin-1), for example, increased the percentage of sinoatrial-like cells, while treatment with retinoic acid pushed the differentiation

toward the atrial lineage. However, these approaches did not allow to obtain a pure population (*Wiese et al., 2011; Gassanov et al., 2004; Hidaka et al., 2003*).

Recently, our laboratory demonstrated that it is possible to isolate a specific population of sinoatrial-like cells on the basis of the expression of CD166 in EBs from mouse embryonic stem cells at a specific time point of differentiation (day 8). CD166, known also as ALCAM (Activated Leucocytes Cell-Adhesion Molecule) or DM-GRASP, is a transmembrane protein, and an adhesion molecule of the Ig superfamily; it is the natural ligand of the human CD6 receptors (*Ibáñez et al., 2006*).

In mice, during heart formation, CD166 is specifically and transiently expressed in the sinus venus, the region from which the SAN develops, (*Hirata et al., 2006; Murakami et al., 2007*). We showed that 24 hours after cell sorting, CD166+, but not CD166-, starts to beat spontaneously. We demonstrated that CD166+ cells, unlike CD166-, express high levels of the specific cardiac markers α-Actinin, cTnI, Mef2c, and GATA4. We also showed that CD166+ cells express Tbx18, Tbx3, Isl-1, and Shox2, which are important for SAN development, and also proteins important in the adult SAN, like ion channels (HCN4, HCN1, CaV1.3, Cav3.2), connexins (Cx30.2), and sarcomeric proteins (ssTnI). Furthermore, CD166+ cells express at very low levels genes typical of the ventricle (Nkx2.5, Kv4.2, HCN2, and Cx43). It was also demonstrated that CD166+ cells express HCN4 at the protein level and they display the I_f current, but also the L- and the T-type calcium currents; CD166+ cells express also β-adrenergic and muscarinic receptors, and could be modulated by isoproterenol and acetylcholine (sympathetic and parasympathetic agonist, respectively). Interestingly, CD166+ cells have a low proliferative potential, don't express markers of pluripotency (Oct4, Nanog, and Rex1), and do not form teratomas *in vivo* (*Scavone at al., 2013*). Therefore in our laboratory it was demonstrated the possibility of isolate a population with the molecular and functional properties typical of sinoatrial cells using CD166 as a marker.

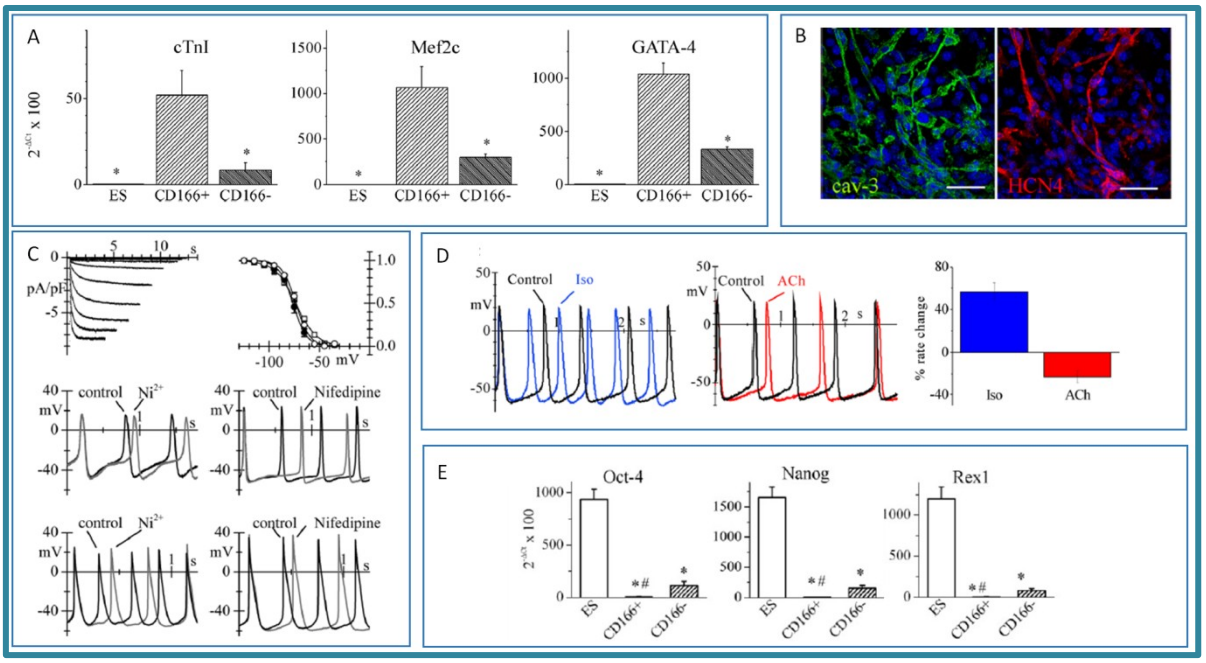

Fig. 12: **(A)** quantitative expression analysis of cardiac genes (cTnI, Mef2c, and GATA-4) in embryonic stem cells (ES) and in CD166+, and CD166- cells sorted at day 8 of differentiation. **(B)** confocal images of CD166+ cells labelled with caveolin-3 (cav-3, green) and HCN4 (red); nuclei were stained with DAPI. **(C)** representative traces of I_f current, recorded from single CD166+ cell, and representative action potentials recorded from both CD166+ cells and SAN cells, in control and under superfusion of 50μmol/L of nickel (Ni^{2+}) and 100nmol/L Nifedipine. **(D)** spontaneous action potentials recorded from CD166+ cells in control and under superfusion of 1μmol/L isoproterenol (Iso) and 0.1μmol/L acetylcholine (ACh); the bar graph shows the mean rate changes caused by the autonomic agonists. **(E)** Quantitative expression analysis of genes of pluripotency (Oct-4, Nanog, and Rex1) in embryonic stem cells (ES) and in CD166+ and CD166- cells sorted at day 8 of differentiation. (*modified from Scavone et al., 2013*).

2.7 Exercise and heart

The cardiovascular benefits of regular exercise are well established and include a better pressure control, improved blood lipid profile, reduced risk of prostate and breast cancer, reduced risk of osteoporosis, increased self-confidence, and it's considered anti-depressant; in addition, exercise is associated with a significant reduction in cardiac events. It is important to underlie that the amount of exercise required to reach these benefits is relatively modest. The current guidelines recommend a minimum of 150 minutes of moderate exercise per week, while professional athletes perform approximately 20 hours of intense exercise. The effects

of chronic endurance exercise may result in a series of cardiac modifications called “athletes heart” that ensure the possibility to sustain the increased cardiac output and metabolic needs of the organism. These cardiac modifications include typical morphological changes (increase in left ventricular wall thickness, increase in both left and right ventricular cavity and in aortic diameter), and a slowing down of the heart rate with significant brady- and tachy-arrythmias. The changes described above are commonly considered benign and generally reversible after detraining, but in the last few years, several studies suggested that endurance exercise could be associated with myocardial remodeling and fibrosis, but also with an increased risk of atrial fibrillation in athletes compared to sedentary people. This idea is supported also by animal studies: for example, Benito and collaborators showed that after 10 weeks of training, rats display fibrosis in atria and ventricles and diastolic dysfunction *(Benito et al., 2011)*. Consequently, extreme high intensity training might not only have physiological but also pathologic consequences, like fibrillation, bradycardia, and atrioventricular conduction abnormalities (*Baldesberger et al., 2008; Sharma et al., 2015; Maron and Pelliccia., 2006*).

Endurance trained athletes are well known to show sinus bradycardia with episodes of resting heart rate lower than 30 beats per minute. Despite bradycardia being considered a physiological condition, it could become pathologic resembling the sinus node disease. As previously described, the setting of heart rate essentially depends on: the intrinsic heart rate, generated by sinoatrial node cell, and by the modulation of the autonomic nervous system. The mechanism at the basis of bradycardia in endurance athletes is controversial, but it is commonly attributed to an increased vagal tone on the pacemaker cells (*Smith et al. 1989; Jensen-Urstad et al. 1997; Coote & White, 2015*). Conversely, using a murine model of endurance, D’Souza and colleagues have recently demonstrated that training-induced bradycardia is not a consequence of an alteration in the autonomic nervous system, but it is due to an intrinsic modification of the heart. In particular, they showed that bradycardia persists (*in vivo*) after blockade of the autonomous nervous system in mice and (*in vitro*) in the isolated heart both in trained mice and rats. They also found no differences in vagal tone of sedentary and trained mice. Furthermore, D’Souza and colleagues demonstrated a reduction of the I_f pacemaker current in sinoatrial node (SAN) cells of trained mice and a reduction of HCN4 (the molecular component of the I_f current) at mRNA and protein level in trained rats. The molecular mechanism

at the basis of this process is not completely understood but they also showed an up-regulation of miR-1, one of the main myomiR, following chronic exercise (*D'Souza et al., 2014*).

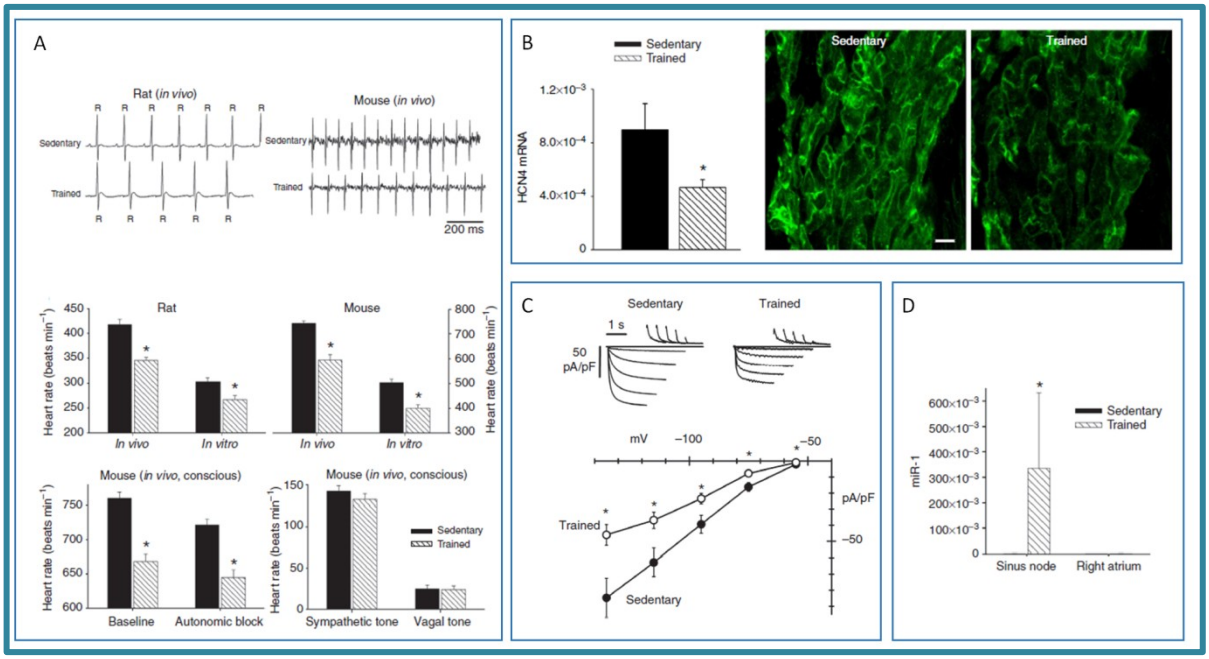

Fig. 13: **(A)** representative ECG traces obtained from sedentary and trained rats and mice; heart rates measured *in vivo* and *in vitro* in sedentary and trained animals (rats and mice); mean heart rate measured *in vivo* in mice at baseline and after complete autonomic block; mean sympathetic tone and vagal tone in conscious sedentary and trained mice. **(B)** downregulation of HCN4 mRNA and protein levels in SAN of trained mice. **(C)** Representative traces and mean current density of I_f current recorded in SAN cells of sedentary and trained mice. **(D)** Mean miR-1 levels in sinus node and right atrium in sedentary and trained mice: miR-1 results up-regulated in SAN of trained mice (*modified from D'Souza et al., 2014*).

2.8 MicroRNA

MicroRNAs (miRNAs) are small non-coding RNAs of 20-25 nucleotides length. They regulate gene expression at post-transcriptional level by annealing to inexactly complementary sequences in the 3'-UTR regions of the target messenger RNA (mRNA). The crucial region for the target recognition is the "miRNA seed" located at the 5' of miRNA and long from 2 to 7 nucleotides (*Lewis et al., 2005; Ha and Kim, 2014*). miRNAs are involved in many physiological and pathological processes, and most of the human coding genes are under their control (*Freidman et al., 2009*). Therefore, miRNAs represent a very important class of gene-regulatory molecules

and consequently, their level and function are strongly regulated at multiple steps, from biogenesis to processing and turnover.

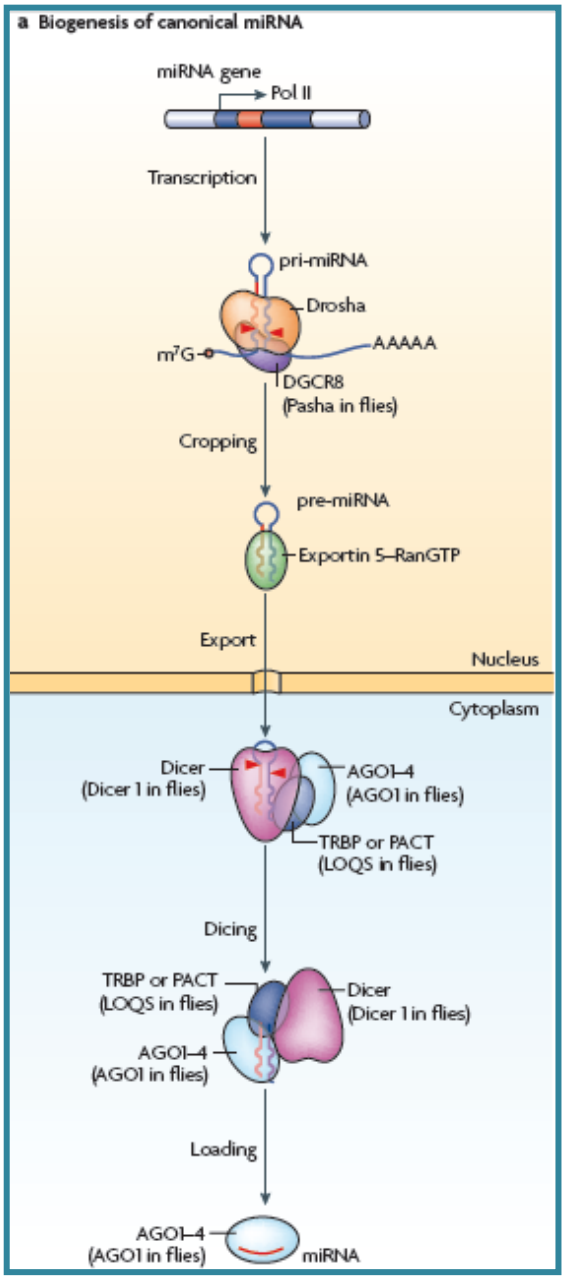

Fig. 14: schematic representation of canonical microRNA biogenesis pathway (*Kim et al., 2009*).

The transcription of the primary transcripts, the pri-miRNAs, is usually mediated by RNA polymerase II (Pol II), from independent genes or from introns of protein-coding genes; the pri-miRNA contains a stem-loop structure of several kilobases. The first step of maturation is mediated by the Microprocessor complex, composed of the RNase III-type Drosha and its cofactor DGCR8, and consists in the cleavage of the

hairpin structures. As a result, there is the formation of the pre-miRNA, a small hairpin. The pre-miRNA is then exported from the nucleus to the cytoplasm, by the exportin 5 (EXP5), where is cleaved by Dicer in proximity of the terminal loop, obtaining a ~22nt miRNA duplex (miRNA/miRNA*), that is loaded into an Ago protein forming, with other cofactors, the RISC effector complex. In this way, Drosha and Dicer determine the two end of future mature miRNA. Probably a helicase removes the unselected strand of the miRNA duplex; the relative thermodynamic stability of the two ends of the duplex has to determine which strand is selected and it is usually the filament with relatively unstable base pairs at the 5' that survives. Generally, most miRNA genes produce one dominant miRNA, but the ratio between the miRNA and miRNA* can vary in different developmental stages or tissues and, since the selection is not a stringent process, miRNAs are sometimes produced from both strands at comparable level. As mentioned before, stringent regulation of miRNA levels is fundamental in order to maintain the cellular functions. One of the first point of regulation is the miRNA transcription, indeed it depends on different transcription factors and epigenetic control; the pri-miRNA processing by Drosha is also considered a regulatory step and depends on many different co-regulatory factors; the RISC assembly is a crucial point due to the presence of different Ago proteins and the miRNA seems to be more stable once assembled into the RISC complex. MicroRNAs are subject to turnover, not only at the mature level, but also at the precursor level, and are controlled by multiple levels of feedback loops (*Kim et al., 2009; Krol et al., 2010; Siomi and Siomi 2010; Ha and Kim, 2014*).

Once incorporated into the silencing RISC complex, a miRNA could pair to a mRNA, and represses it by inhibiting translation and/or inducing degradation of the target mRNA (*Selbach et al., 2008*). A single miRNA could regulate the expression of hundreds of genes because it binds 3'UTR of different mRNA targets with a perfect or an imperfect complementarity.

2.9 myomiR and miR-1

microRNAs are expressed in all tissues, and miRNA specifically expressed in muscle cells are known as myomiR. The myomiR family is composed of miR-1, miR-133a, miR-206, miR-208a, miR-208b, miR-499, and miR-486 (Fig. 15). They are expressed

both in heart and skeletal muscle, except miR-208a, which is cardiac specific (*McCarthy, 2011*).

MyomiR	Host Gene	Expression Pattern	Knockout Phenotype	Study
MiR-1-1	*Mib1*	Heart, skeletal muscle	No knockout	—
MiR-1-2	Intergenic	Heart, skeletal muscle	50% lethal, cardiac defect	Zhao *et al.*, 2007 (38)
MiR-133a-1	*Mib1*	Heart, skeletal muscle	No overt phenotype	Liu *et al.*, 2008 (22)
MiR-133a-2	Intergenic	Heart, skeletal muscle	No overt phenotype	Liu *et al.*, 2008 (22)
MiR-206	Intergenic	Skeletal muscle (Type I)	No overt phenotype	Williams *et al.*, 2009 (37)
MiR-208a	*Myh6*	Heart	Blunted stress response	van Rooij *et al.*, 2007 (36)
			Conduction defects	Callis *et al.*, 2009 (5)
MiR-208b	*Myh7*	Heart (low), skeletal muscle (Type I)	No overt phenotype	van Rooij *et al.*, 2009 (35)
MiR-486	*Ank1*	Heart, skeletal muscle	No knockout	—
MiR-499	*Myh7b/14*	Heart, skeletal muscle (Type I)	No overt phenotype	van Rooij *et al.*, 2009 (35)

Fig. 15: myomiR: muscle-specific microRNA (*McCarthy, 2011*).

Recent studies demonstrate that myomiR are involved in different aspects of muscle and heart function, in particular they are involved in myoblast proliferation, differentiation, and contractility and in different heart diseases like, cardiac hypertrophy, heart failure, and arrhythmias. For example, miR-133 seems to promote myoblast proliferation and it is linked to cardiac arrhythmias inhibiting the expression of HERG, the molecular component of the repolarizing current I_{Kr}; miR-208 is involved in a switch from α- to β-MHC, in cardiac hypertrophy and fibrosis. (*van Rooij et al., 2008*).

miR-1 is one of the main myomiR and the most abundant miRNA in human and mouse heart; miR-1 starts to be expressed in mouse heart at day 8.5 of development with a strong increase after birth (*Lagos-Quintana et al., 2002*).

miR-1 is encoded by two genes (miR-1-1 and miR-1-2): miR-1-1 is located into the intron 2 of an uncharacterized gene on chromosome 20, while miR-1-2 is located into the intron 12 of the MIB1 gene on chromosome 18. Although separate genes encode miR-1-1 and miR-1-2, they are identical in sequences. Deletion of miR-1-1 or miR-1-2 results in an analogue phenotype in mice: incompletely penetrant lethality, cardiomyocytes proliferative defects, and electrophysiological abnormalities; while the double knock-out is lethal before weaning. miR-1-null cardiomyocytes have abnormal sarcomere organization (*Zhao et al., 2007; Heidersbach et al., 2013*). Over-production of miR-1 during heart development in mouse results in defective ventricular myocytes proliferation (*Callis and Wang, 2008*).

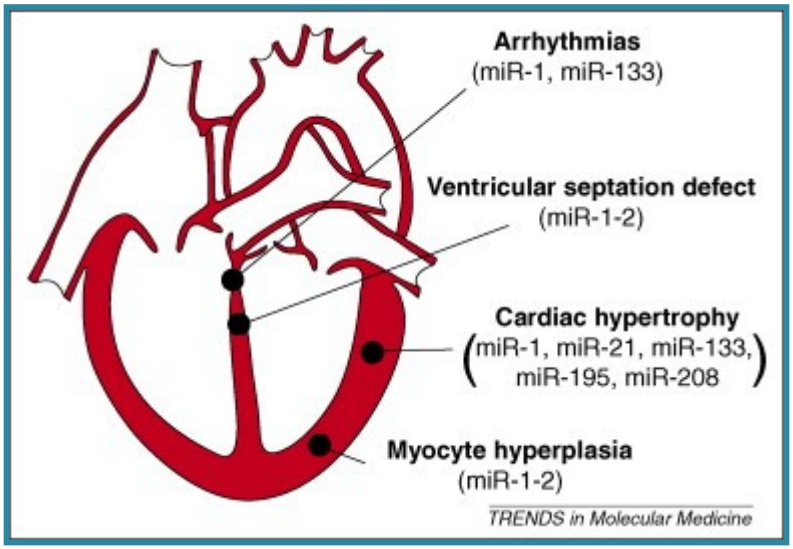

Fig. 16: miRNA roles in heart development and function. miR-1 is involved in arrhythmias, defective ventricular septation, cardiac hypertrophy and myocytes hyperplasia (*Callis and Wang, 2008*).

miR-1 was also shown to be involved in differentiation of mouse and human embryonic stem cells in embryoid bodies (EBs) which recapitulate embryonic development; in particular, miR-1, together with miR-133, promotes the mesoderm formation and they are potent repressor of non-muscle gene expression, suppressing the ectodermal and mesodermal differentiation. During the following stages of differentiation, miR-1 has opposite effects compared to miR-133, indeed miR-1 promotes both cardiac and skeletal muscle differentiation, while miR-133 inhibits them (*Ivey et al., 2008*).

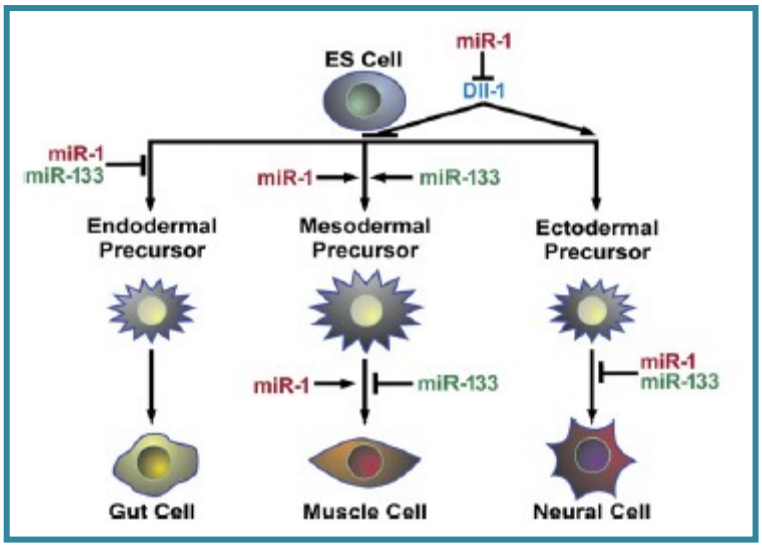

Fig. 17: role of miR-1 and miR-133 during mESCs differentiation (*Ivey et al., 2008*).

It was demonstrated that different microRNAs could regulate cardiac excitability and arrhythmogenesis, in particular abnormal expression of miR-1 seems to be involved in cardiac arrhythmias and atrial fibrillation (AF), even though their role is still controversial: miR-1 is reduced in samples of AF patients, while results increased in samples from patients with coronary artery diseases. It was also demonstrated that reduction of miR-1 levels significantly reduces arrhythmias in rats infarcted myocardium, while injection of miR-1 promotes it. It is well known that AF is characterized by electrical remodeling due to ion channels alterations and structural remodeling, and it was demonstrated that miR-1 also regulates, directly or indirectly, the expression levels of some ion channels (HCN2, HCN4, KCNJ2, KCND2) and the level of connexin 43, reinforcing the idea that miR-1 could be involved in cardiac arrhythmogenesis (*Girmatsion et al., 2009; Duan et al., 2014; Yang et al., 2007; Santulli et al., 2014*).

miR-1 is also involved in cardiac remodeling and in particular in cardiac hypertrophy, myocardial infarction and heart failure. The miR-1 levels are down-regulated in different kinds of cancer like rhabdomyosarcoma, lung, bladder and prostate cancer (*Li et al., 2014).*

2.10 miR-423

miR-423 is located in a region of chromosome 17q11.2. It was demonstrated that miR-423-5p is a suitable circulating biomarker for heart failure (HF), and its upregulation in blood of patients with HF is associated with an upregulation of miR-423 in failing myocardium, suggesting that the increased circulating miR-423 is derived from the myocytes (*Tijsen et al., 2010*). Miyamoto and coworkers analyzed the levels of miR-423-5p in human serum and in pericardial fluid (PF) and they found that its level is significantly higher in PF than in serum. Furthermore, they found that the levels of miR-423 are elevated in serum of patients with unstable angina pectoris compared with those of patients with stable angina pectoris or patients with aortic valve replacement due to aortic stenosis (*Miyamoto et al., 2015*). Bauters and collaborators found that miR-423 is not a useful marker for myocardial infarction (*Bauters et al., 2013*). Li and coworkers demonstrated that miR-423-5p is dramatically increased in patients with dilated cardiomyopathy, and its introduction in

human cardiomyoblasts reduces the proliferation and induces apoptosis. They also found Grb-associated binders 1 (Gab 1) as potential target using a luciferase assay (*Li et al., 2016*).

miR-423-5p was also found upregulated in colon cancer stem cells and a single nucleotide polymorphism (SNP) in pre-miR-423 was associated with breast cancer (*Zhang et al., 2011; Wang et al., 2013; Zhao et al., 2015*).

3. Aim

Endurance athletes display structural and functional cardiac modifications with the most common being sinus bradycardia. D'Souza and coworkers demonstrated in trained animal models (mice and rats) that this sinus bradycardia is due to an intrinsic modification of the cellular pacemaking mechanism, rather than a modification of the vagal tone on the heart (*D'Souza et al., 2014*). In particular, they found that in SAN cells of trained mice there is a reduction of the funny current, the main contributor to the slow diastolic depolarization (*DiFrancesco et al., 1986 b*); they also demonstrated an upregulation of miR-1, one of the muscle-specific miRNA (myomiR) in the SAN of trained mice (*D'Souza et al., 2014*). Preliminary unpublished data from our collaborators in Manchester also indicated an up-regulation of miR-423 in SAN of trained mice. Both miR-1 and miR-423 directly bind the 3'UTR of HCN4 channels, the molecular constituent of the funny current. Starting from this evidence, the aim of our work is to evaluate the specific effects of miR-1 and miR-423 up-regulation in sinoatrial-like cells obtained from mESCs.

4. Methods

4.1 Plasmids

In order to obtain the mESC lines overexpressing the microRNAs of interest, we used three different constructs within the same plasmids (Fig. 18). The plasmid contained the miRNA of interest (or no miRNA as a control), the eGFP sequence under the same constitutive promoter (CMV), and the puromycin and ampicillin resistant cassette.

All plasmids are a kind gift of the Professor Mark Boyett, from the University of Manchester, and derived from GeneCopeia.

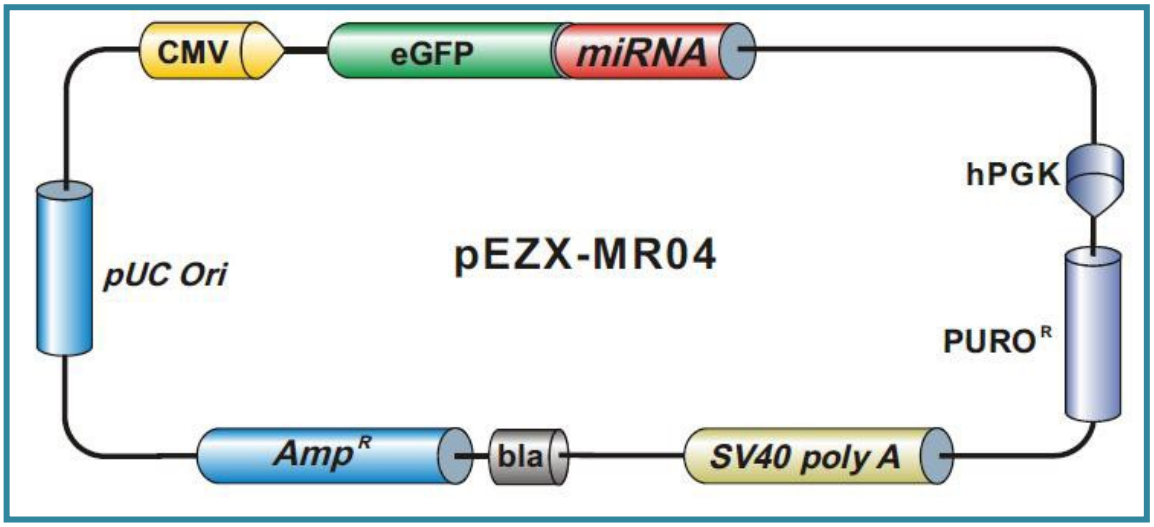

Fig. 18: general map of the plasmids, used for the overexpression of miR-1, miR-423 and the empty vector as control.

4.2 Plasmidic DNA extraction

Competent E. Coli cells were transformed with the three different plasmids. Bacteria were grown in culture LB (Luria Bertani) medium at 37°C with constant shaking over-night. Ampicillin at the concentration of 50µg/mL was added to the LB medium.

Plasmids were isolated using the commercial kit *NucleoSpin® Plasmid Mini Prep Macherey-Nagel®* as follows. 5mL of saturated E.Coli LB culture were centrifuged at 4'000xg for 15 minutes. Once discarded the supernatant, the pellet was

resuspended in 250µL of Buffer A1 and then 250µL of buffer A2 were added and mixed gently. At the end of 5 minutes of incubation at room temperature, 300µL of buffer A3 were added and mixed thoroughly; the solution was centrifuged for 5 minutes at 11'000xg at room temperature. The supernatant was transferred into a NucleoSpin® Plasmid Column and subsequently centrifuged for 1 minute at 11'000xg. The flow-through was thrown away, 600µL of buffer A4 were added to the column and centrifuged for 1 minute at 11'000xg and the flow-through discarded again. The column was centrifuged another time for 2 minutes at 11'000 x g and then the column was placed in a new collection tube and the DNA was eluted in 50µL of milliQ water centrifuging for 1 minute at 11'000xg.

4.3 mESC culture

Mouse embryonic stem cells (mESC; D3 line, ATCC) were cultured in feeder-free condition in culture medium contained KO-DMEM (Gibco), 15% Knock-Out Serum Replacement (Gibco), 0.1 mM Non Essential Amino Acids (Sigma-Aldrich), 0.1mM β-mercaptoethanol (Sigma-Aldrich), 2mM L-glutamine (Sigma-Aldrich), 10^3U/ml Leukemia Inhibitory Factor (LIF, GeneSpin), 100U/ml Penicillin and 0.1mg/ml Streptomycin (Sigma-Aldrich). Cells were splitted two times in a week, using Tryple Express (Gibco) in order to avoid an excessive growth and uncontrolled differentiation.

4.4 mESC electroporation

Three batches of $2x10^6$ mESC were electroporated with the proper plasmid: one containing the miR-1 sequences, one containing the miR-423 sequences, and the empty vector as control. The electroporation procedure was carried out using a commercial kit composed by 82µL of Nucleofector solution and 18 µL of Supplement (Lonza) to which we added 10µg of plasmid with a concentration between 1 and 5 µg/µL. We used the electroporator Nucleofactor® II (Amaxa Byosystems) with the A24 program, specific for embryonic stem cells. Once electroporated, cells were kept

in stringent selection for 2 weeks with puromycin 1µg/mL. Non-electroporated cells were treated with the same concentration of puromycin as control.

4.5 Selection of eGFP positive cells

Colonies of mESCs were divided with Tryple Express, centrifuged, resuspended in culture medium, and filtered through a 70µm syringe filcons (BD Biosciences) , in order to obtain a homogeneous suspension of single cells. This procedure was repeated for each cell line. Cells obtained were analyzed using a cytometer (BD FACS Aria II), mESCs D3 were used to set the basal fluorescence, and the resulting eGFP positive cells were sorted to isolate only the cells where the plasmid was properly integrated.

4.6 Differentiation of mESCs in cardiomyocytes

ES cells were differentiated using the Hanging Drop technique, previously described by Maltsev (*Maltsev et al., 1993*). The hanging drops, containing ~500 cells in 20µL of differentiating medium ($2.5x10^4$ cellule/mL), were cultured for 2 days hanged in bacterial dishes up side down and then grown for further 5 days in the plate flooded with differentiating medium. 7 day-old Embryoid Bodies (EBs) were plated on tissue culture dishes coated with gelatin 0.1% (Type B, Sigma) in differentiating medium.

The differentiating medium contains: DMEM (Gibco), 4mM L-glutamine (Gibco), 0.1mM Non Essential Amino Acids (Sigma-Aldrich), 0.1mM β-mercaptoethanol (Sigma-Aldrich), 20% Fetal Bovine Serum (FBS) (Gibco), 1mM Sodium Pyruvate (Sigma-Aldrich), 100U/ml Penicillin, 0.1mg/ml Streptomycin.

EBs usually displayed spontaneous beating activity at day 7 of differentiation, proving the proper differentiation and presence of cardiomyocytes.

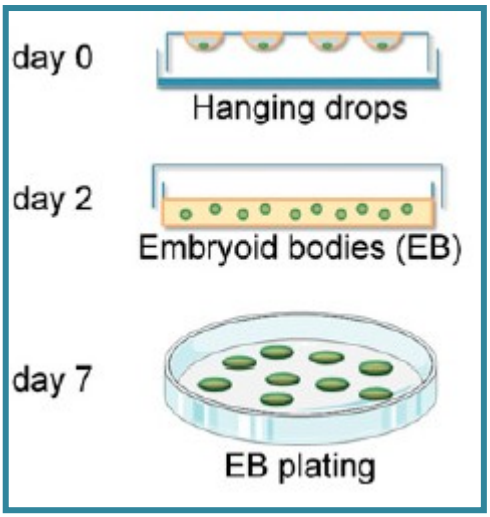

Fig. 19: schematic representation of mESCs differentiation using the Hanging Drop technique. (Modified from *Barbuti and Robinson, 2015*)

4.7 Selection of CD166+ cells using a cell sorter

At day 8 of differentiation the EBs were detached from the plate and collected in a tube and allowed to sediment on the bottom by gravity. They were then washed two times with PBS (Phosphate Buffered Saline) and, after 10 minutes of incubation in presence of Tryple express at 37°C with constant shaking, they were mechanically dissociated to single cells. Cells were suspended in a solution of PBS with 1mM $CaCl_2$, 10% FBS, and 5mM EDTA, and subsequently counted.

Cells were incubated with the PE-conjugated rat anti-mouse CD166 antibody (eBioscience) for 30 minutes at 4°C under constant shaking, using 2.5µg of Ab for 10^6 cells. $3x10^5$ cells were incubated with the corresponding isotype (PE rat IgG). At the end of the incubation, cells were washed twice with the solution of PBS with 1 mM $CaCl_2$, 10% FBS, and 5mM EDTA, and then resuspended in the same solution. Finally, they were filtered with 70µm syringe filcons for the subsequent FACS analysis. Using the cell sorter CD166+ and CD166- cells were separated and used for the subsequent analysis.

For the electrophysiological experiments, cells were put to re-aggregate for 24 hours in 1mL of differentiating medium in a low adhesion bacterial dishes, inclined at 45°, and then plated in a silicon support in a cell culture dish at the density of 10^5 cells/mm^2 in 15µL of differentiating medium. Around the silicon support, we added 1mL of differentiating medium to prevent the evaporation of the 15µL of medium.

After 4 hours the silicon support was removed, and the medium increased to 2mL. The medium was changed every 24/48 hours, until the electrophysiological analysis.
To obtain single cells to perform voltage clamp experiments, we dissociated the aggregates of sinoatrial-like cells (CD166+) using 100µL of Trypsin-EDTA (Sigma-Aldrich) diluted 1:2 with PBS. Dissociation was performed in subsequent steps, and the isolated cells obtained from each step were plated in a cell plate with a diameter of 35mm, previously filled with 2mL of differentiation medium with Ara-C. Medium was changed after 6 hours from dissociation.

4.8 Isolation of sinoatrial node from mice

Sinoatrial nodes (SAN) were isolated from 10 month-old female mice.
The heart, quickly removed, was placed in cold Tyrode solution (mM: NaCl, 140; KCl, 5.4; CaCl2, 1.8; MgCl2, 1; D-glucose, 5.5; Hepes-NaOH, 5; pH 7.4) containing 1000 units of heparin to prevent blood clots formation, and the SAN tissue was dissected and conserved in liquid nitrogen until the RNA isolation. Animal protocols conformed to the guidelines of the care and use of laboratory animals established by Italian (DL. 26/2014) and European (2010/63/UE) directives.

4.9 RNA Extraction

Tissues were resuspended in 1mL of TRIzol Reagent (Life technologies) and put into a potter to be mechanically homogenized and then further processed through the needle of an insulin syringe. After that, the protocol required the following steps:

1. The tube was centrifuged for 10 minutes at 12’000xg at 4°C;
2. The supernatant was moved into a new tube;
3. 200µL of chloroform-isoamyl-alcohol (Sigma) were added;
4. The tube was inverted 10 times and kept 4 minutes at room temperature (RT);
5. The tube was centrifuged for 20 minutes at 12’000xg at 4°C, at the end of the centrifuge there was the formation of three phases: at the top a colorless aqueous phase with the RNA, in the middle an interphase with DNA, and at the bottom a red phase with proteins and lipids;

6. The aqueous phase was transferred in a new tube, where an equivalent volume (400-500µL) of isopropanol and 1µL of glycogen was added;
7. The tube was inverted ten times and then the RNA was precipitated 10 minutes at RT or overnight at -20°C;
8. The tube was centrifuged for 20 minutes at 12'000xg at 4°C, and at the end of the centrifuge a RNA pellet formed at the bottom of the tube;
9. The RNA pellet was washed with 1mL of ethanol at 75%;
10. The tube was centrifuged for 10 minutes at 7'500xg at 4°C;
11. The ethanol was removed and the tube allowed to dry;
12. The RNA pellet was resuspended in milliQ water and quantified using a spectrophotometer.

For RNA extraction cells were resuspended in 1mL of TRIzol Reagent and then mechanically homogenized through the needle of an insulin syringe. The protocol was continued from step 3 above.

4.10 DNase treatment

The RNA was treated with DNase I (Thermo Scientific) in order to remove any presence of genomic DNA. 1µg of RNA was treated with 1µL of DNase I (1U/µL), in a solution of $MgCl_2$ in a final volume of 10µL of milliQ water.
After 30 minutes at 37°C 1µL of EDTA 25mM (Thermo Scientific) was added and then put at 65°C for 10 minutes.
The RNA was stored at -80°C.

4.11 Reverse transcription from RNA to cDNA for miRNAs

A specific reverse transcription kit from Qiagen® was used to evaluate the microRNAs levels in the RNA samples. miRNA were prepared as described in the table 1 and treated for 60 minutes at 37°C and for 5 minutes at 95°C.

	Quantity
RNA	250ng
miR-39 Solution Work ($1.6x10^8$ copies/µL)	2.20µL
High Specific Buffer 5X	4µL
miR Script Nucleics Mix 10X	2µL
miR Script RT Mix 10X	2µL
milliQ Water	To the final volume of 20µL

Tab. 1: mix for miRNA reverse transcription.

In the mix the miR-39, an exogenous miRNA from C. elegans, was added to be used as normalizer during the subsequent real-time PCR.

During the reverse transcription the “NO RNA” was prepared as the control of the reaction, replacing the RNA sample with milliQ water.

4.12 Reverse transcription from RNA to cDNA for mRNAs

For the study of mRNA expression, the reverse transcription was carried out using a commercial kit (Thermo Scientific). Samples were prepared as described in the table 2 and incubated for 10 minutes at 25°C, for 15 minutes at 50°C and for 5 minutes at 85°C.

	Quantity
RNA	1µg
Reaction Mix 5X	4µL
Maxima Enzyme 10X	2µL
milliQ Water	To the final volume of 20µL

Tab. 2: mix for mRNA reverse transcription.

During the reverse transcription the “NO RNA” was prepared as control of the reaction, replacing the RNA sample with milliQ water.

4.13 Real-Time qPCR

The cDNAs obtained were analyzed using quantitative real-time PCR, (Line-gene9600, Bioer). Each sample was analyzed in a technical triplicate and in each real-time the “NO RNA” and the “NO DNA” (a qPCR sample with milliQ water instead of cDNA) were analyzed as negative controls. All the data were expressed as $2^{-\Delta Ct}$x100±SEM.

miRNA expression:

The qPCR for micrRNA was performed using the mix indicated in table 3 for each sample. Expression of miR-1 and miR-423 were normalized on miR-39 expression.

	Quantity
cDNA	2.5ng
Universal Primer 10X	2.5µL
Primer miR 10µM	1.25µL
QuantiTect SYBER Green PCR master Mix 2X	12.5µL
milliQ Water	To the final volume of 25µL

Tab. 3: mix for real-time qPCR (miRNA).

The forward primers were specific for each microRNAs analyzed (Tab. 4), while the reverse primer was the same and was the “Universal Primer” provided in the kit.

miRNA	**FWD PRIMER**
mmu -miR-1a-1-3p	TGGAATGTAAAGAAGTATGTAT
mmu -miR-423-5p	TGAGGGCAGAGAGCGAGACTTT
miR-39	TCACCCGGGTGTAAATCAGCTTG

Tab. 4: miRNA Primers (Sigma-Aldrich).

The PCR conditions were:

- 95°C for 15 minutes
- 94°C for 15 seconds
- 55°C for 30 seconds
- 70°C for 30 seconds

The last three stages were repeated for 50 cycles, and the last one was the detection stage.

mRNA expression:

The qPCR for mRNA was performed using the mix indicated in table 5 for each sample. Expression of different genes were normalized on the expression of GAPDH (Glyceraldehyde 3-phosphate dehydrogenase).

	Quantity
cDNA	10ng
Forward Primer 10X	1.25µL
Revers Primer 10µM	1.25µL
SYBER Green 2X	12.5µL
milliQ Water	To the final volume of 25µL

Tab. 5: mix for real-time qPCR (mRNA).

The forward and the reverse primers are listed in the table 6.

Gene	FORWORD PRIMER	FORWORD PRIMER
HCN4	GTCGGGTGTCAGGCGGGA	GTGGGGGCCACCTGCTAT
α-Act	GCGGATATCGATGTCACAC	AAACTGTGTTACGTCGCCC
Tbx18	TGATGGCCTCCAGAATGC	CCGAGACTCTGGGAGGAAC
Shox2	GAAAGGACAAGGGCGTCAC	AACGTAGGTGCTTTAAGGATGC
Oct4	CTCCTTCTGCAGGGCTT	GTTGGAGAAGGTGGAAAC
Rex1	GGGCACTGATCCGCAAAC	CAGCAGCTCCTGCACACAGA
GAPDH	TGTAGACCATGTAGTTGAGGTCA	AGGTCGGTGTGAACGGATTTG

Tab. 6: primers (Sigma-Aldrich) used for real-time qPCR.

The PCR conditions were:

- 95°C for 15 minutes
- 95°C for 15 seconds
- 60°C for 30 seconds
- 72°C for 30 seconds

The last three stages were repeated for 45 cycles, and the last one was the detection stage.

4.14 Electrophysiological Analysis

Our standard patch-clamp setup includes:

- Inverted microscope (Axiovert S100) positioned on an anti-vibration table.
- Patch-clamp amplifier (Axopatch 200B, Axon Instruments).
- Digital interface (Digidata 1550B, Axon Instruments).
- Micromanipulators.
- Solution temperature control.
- pClamp 10.6 software (Axon Instruments).

All the electrical devices were positioned inside a Faraday's cage, to shield from electrical noise.

Electrophysiological experiments were performed using glass pipettes with a resistance of about 5-8mΩ when filled with a solution containing (): K-Aspartate, 130 mmol/L; NaCl, 10 mmol/L; EGTA-KOH, 5 mmol/L; CaCl2, 2 mmol/L; MgCl2, 2 mmol/L; ATP (Na-salt), 2 mmol/L; creatine phosphate, 5 mmol/L; GTP (Na-salt), 0.1 mmol/L; pH 7.2.

Electrophysiological protocols were designed with pClamp software. All data were acquired with pClamp software and an Axopatch 200B amplifier. To record the capacitive current, we used a protocol with a single hyperpolarizing step of 10 mV amplitude (from -35 to -45mV) for 30 ms of duration.

Action potentials were recorded in current-clamp configuration during the perfusion of Tyrode solution. The extracellular solution used to record the I_f current was Tyrode with the addition of $BaCl_2$ (1μM) and $MnCl_2$ (2μM) to improve I_f dissection over other ionic components.

The activation curve of I_f current was obtained by hyperpolarizing steps to the range -35/-125mV, followed by a fully activating 1.5s step at -125mV, from a holding potential of -35mV. The duration of the first step was decreased as the activation of the current became progressively faster. Current amplitudes were normalized for the cell capacitance to obtained current densities (pA/pF). After normalization to maximum amplitude, tail currents measured at -125mV were fitted using Boltzmann equation:

$$y = \frac{1}{1 + e^{\frac{V - V_{1/2}}{s}}}$$

- “V”: voltage.
- “y”: fractional activation.
- “V1/2”: half activation voltage.
- “s”: inverse-slope factor.

4.15 Immunofluorescence Analysis

The immunofluorescence protocol consisted in:

- 30 minutes of fixation with 4% paraformaldehyde (Sigma-Aldrich) at 4°C;
- Two washes of 10 minutes with PBS supplemented with Glycine (0.1M);
- 30 minutes of permeabilization at RT, with PBS and 1.5% Triton (Sigma-Aldrich);
- One hour of block with PBS with 1% BSA (Sigma-Aldrich), 0.3% Triton, and 10% serum;
- Incubation over night with primary antibodies (Tab. 7), in a solution of PBS with 1% BSA, 2% serum, and 0.1% Triton, in a wet chamber;
- Three washes of ten minutes each one with PBS;
- One hour of incubation with the secondary antibodies (Tab. 8), in a solution of PBS with 1% BSA, 2% serum, and 0.1% Triton, in a wet chamber;
- Three washes of ten minutes each one with PBS;
- 30 minutes of incubation with DAPI (4' 6-diamidino-2-phenylindole), at RT;
- Two washes of three minutes each with PBS;
- At the end the cover glass was assembled with the Fluorescent Mounting Medium (Dako) and fixed with clear nail polish.

The fluorescence images were acquired using a Video Confocal microscope (ViCo, Nikon).

Primary antibody	Dilution
Rabbit anti-HCN4 (AlomooneLabs)	1:100
Mouse anti-α-Act (Sigma-Aldrich)	1:1000

Tab. 7: primary antibodies, and dilution used.

Primary antibody	Dilution	Fluorophore
Donkey anti-mouse (Molecular Probes)	1:500	Alexafluor 488
Donkey anti-rabbit (Molecular Probes)	1:500	Alexafluor 594

Tab. 8: secondary antibodies, and dilution used.

4.16 Isolation of Neonatal rat ventricular cardiomyocytes

The ventricular myocytes were isolated from 3-day-old neonatal CD1 rats.

Animals were sacrificed and the heart removed and kept in PBS at 4°C. Once removed the atria, ventricles were chopped in small pieces and put in an enzymatic solution; 300µL of solution were used for each heart (ADS 1X: NaCl 116.4mM; KCl 5.4mM; NaH_2PO_4•H20 1mM; $MgSO_4$•H20 0.8mM; HEPES 20mM; Glucose 5.5mM; Collagenase I 136U/mL; Pancreatin 0.4mg/mL; pH 7.4).

After 20 minutes of digestion at 37°C under constant shaking, the solution containing the cells was removed, and diluted with 1mL of FBS for each heart and centrifuged at 310xg for 5 minutes. Once discarded the supernatant, the pellet of cells was

resuspended in FBS and conserved in ice. The procedure was repeated at least 5-6 time. At the end of all digestion cells were centrifuged again and resuspended in maintaining medium (M199; 10% Horse Serum; 5% FBS; 100U/mL Penicillin; 0.10mg/mL Streptomycin; 2mM L-glutamine), and plated two times in a cell culture plate (diameter 100mm) for 40 minutes, to enrich the number of cardiomyocytes exploiting the capacity of fibroblasts to attach faster to the plate. After these two pre-plating, the cells were counted and 800'000 cells were put in each plate of 35mm.
To reduce fibroblasts proliferation 2.5μM arabinofuranosyl Cytidine (Ara-C, Sigma-Aldrich) was added to the medium. The day after the isolation the percentage of Horse Serum was reduced from 10% to 5%.

4.17 Transfection of neonatal rat ventricular cardiomyocytes

The day after the isolation, cardiomyocytes were transfected with the plasmid containing the miR-423 sequence and, in parallel, with the empty plasmid using Lipofectamine® 2000 (Life Technologies) using the following protocol: the mix A (242.5μL of Opti-MEM and 7.5μL of Lipofectamine) was prepared in a low adhesion tube and, after 5 minutes, the mix B (1.5μg of plasmid in a final volume of Opti-MEM of 250μL) was added. After 20 minutes, 500μL of the final mix and 1.5mL of medium were added to the plates containing the cells.
36 hours after the transfection, to obtain small aggregates of cells, cardiomyocytes were enzymatically digested with Trypsin for 2-3 minutes at 37°C and then mechanically dissociated; after 5 minutes of centrifuge at 310xg cells were resuspended in the maintaining medium and plated at the right density. Since the plasmid presents both the eGFP and the miRNA sequences under the control of the same promoter, cells expressing the green fluorescent protein were used for the electrophysiological experiments.

5. Results

5.1 miR-1 and miR-423 directly binds the 3'UTR of HCN4 mRNA

Our collaborators in Manchester demonstrated that miR-1 and miR-423 are both up-regulated in the SAN of trained mice, and that the heart of trained mice display intrinsic bradycardia. Mice were trained for 4 weeks by a swimming protocol of 60 minutes twice in a day. Knowing that the I_f current is mediated by the HCN4 channels in SAN cells, and that it is fundamental for the setting of the heart rhythm, they investigated if these two microRNAs could regulate HCN4 expression. To do this, they performed a luciferase reporter assay: the HCN4 3'UTR region was cloned in a plasmid in frame with the luciferase sequence. In case of binding of the miRNA to the 3'UTR, we expect a reduction of the luciferase transcription and thus of its activity. As shown in figure 20, our collaborators demonstrated that both miR-1 and miR-423 directly bind to the 3'UTR of HCN4 channels.

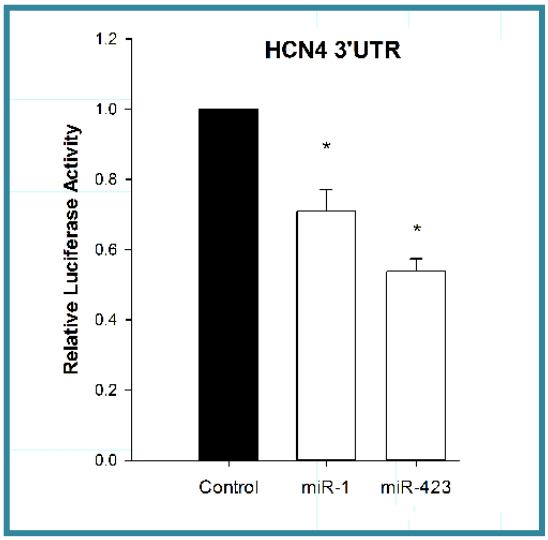

Fig 20: bar graph of luciferase report assay: miR-1 and miR-423 lead to a reduction of the luciferase activity and so it is possible to conclude that they directly bind the 3'UTR of HCN4 channels.

5.2 Generation of mESC lines stably overexpressing miR-1 and miR-423

In order to study the effects of miR-1 and miR-423 overexpression on the electrophysiological properties of pacemaker cells, we need to transfect cells with plasmids containing the miRNA of interest under the control of a strong promoter. Only the last year, it was demonstrated that it is possible to keep in culture sinoatrial cells isolated from adult mice, and that it is possible to infect, but not transiently transfect them. Moreover, in this way, it is possible to obtain and analyze just a little number of cells (*St. Clair et al., 2015*). Consequently, we decided to study the role of these two microRNAs in sinoatrial-like cells isolated from 8 day-old Embryoid Bodies (EBs) obtained from engineered mESCs, following a specific protocol developed in our laboratory (*Scavone et al., 2013*).

To obtain sinoatrial-like cardiomyocytes overexpressing miR-1 and miR-423, three batches of mESCs were electroporated with three different plasmids: one containing the miR-1 sequence, one containing the miR-423 sequence under the control of a strong constitutive promoter (CMV) and the corresponding empty plasmid. Thanks to the presence of the puromycin resistance cassette, cells were kept under stringent antibiotic selection (1µg/mL) for at least two weeks in order to induce integration of the plasmid into the genome. After this stringent selection, the antibiotic concentration was lowered to 0.5µg/mL for maintenance. The effect of puromycin selection was checked on non-electroporated mESCs (mESC-D3), which all died after 24-48 hours of selection.

Since the miRNA-containing plasmids have also the eGFP under the same promoter, two weeks after the puromycin selection, we isolated only eGFP-positive cells, using a cells sorter, in order to obtain only a population of cells in which the plasmid is properly integrated.

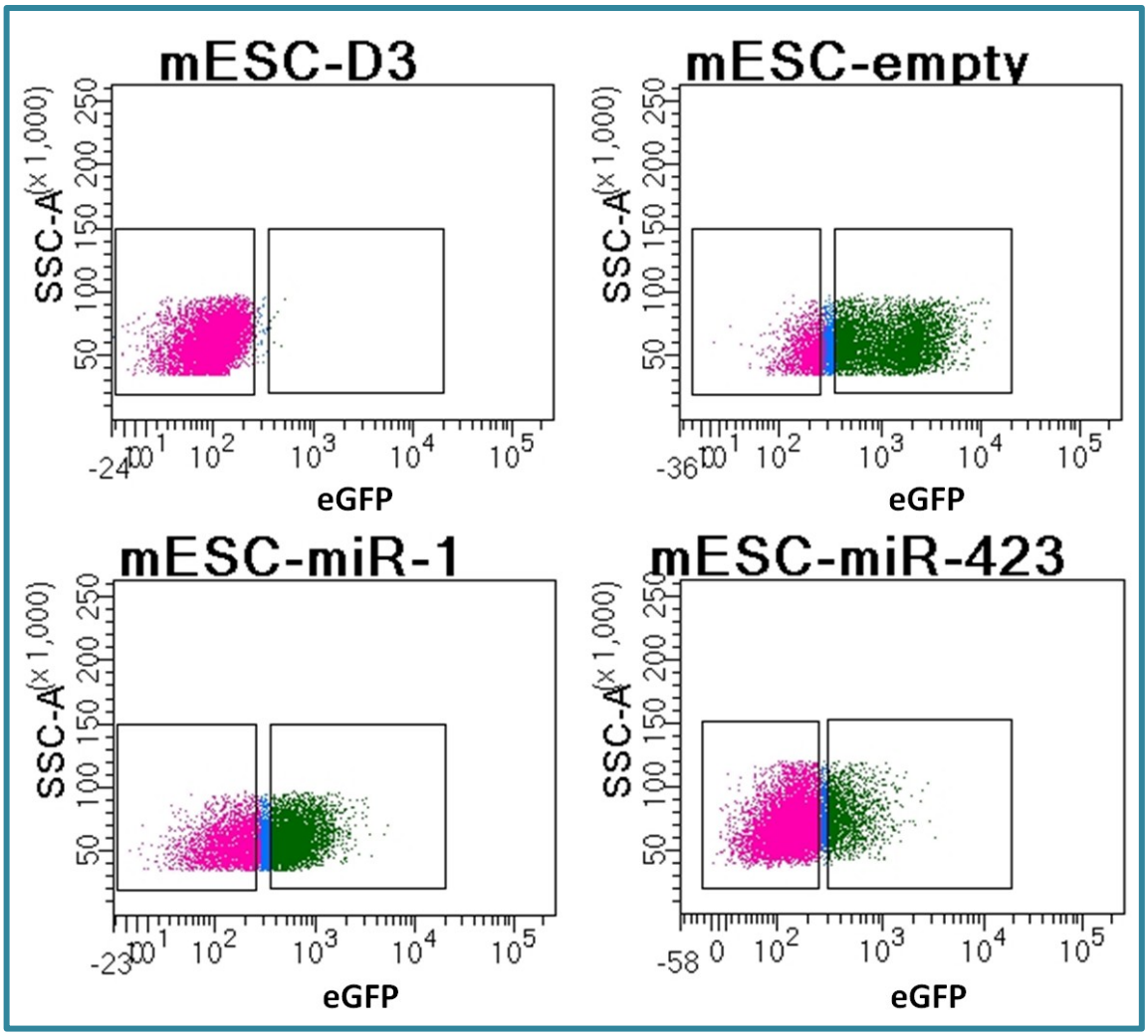

Fig 21: representative flow cytometer analysis (dot plots) of eGFP positive cells derived from non-electroporated mouse embryonic stem cells (mESC-D3), mouse embryonic stem cells electroporated with the miR-1 plasmid (mESC-miR-1), mouse embryonic stem cells electroporated with the miR-423 plasmid (mESC-miR-423), and mouse embryonic stem cells electroporated with the empty plasmid (mESC-empty).

At the end of this procedure, we evaluated the effective overexpression of miRNAs using real-time quantitative PCR: as evident from the bar graph of Fig. 22 miR-1 is more than $2x10^4$ times up-regulated in ES cells electroporated with the miR-1 plasmid compared to those electroporated with the empty vector (mESC-miR-1 35.12±5.64 vs mESC-empty $2.2*10^{-4}$±$6.5x10^{-4}$; n≥6), while miR-423 results ~3 times up-regulated in ES cells electroporated with the miR-423 plasmid compared to those electroporated with the empty vector (mESC-miR-423 5.17±0.40 vs mESC-empty 1.91±0.59; n=4).

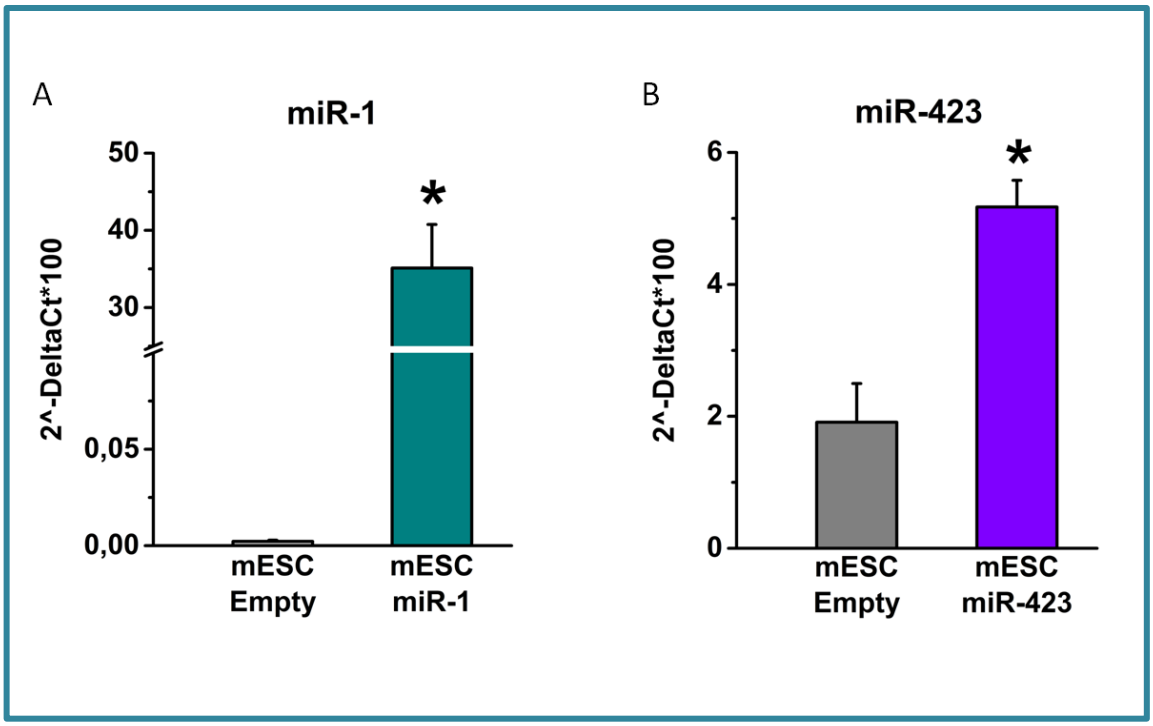

Fig 22: **(A)** mean expression of miR-1 in mESC-empty (grey, n=6) and in mESC-miR-1 (green, n=7). **(B)** Mean expression of miR-423 in mESC-empty (grey, n=4) and in mESC-miR-423 (purple, n=4). Note the difference in the y scale. * p<0,05 (t-test).

This protocol allows to obtain for each transfection, one stable cell line: the first one overexpressing miR-1 (mESC-miR-1), the second overexpressing miR-423 (mESC-miR-423), and the last one containing the empty vector that will be used as a control (mESC-empty) during subsequent analysis.

Afterwards, we evaluated the expression levels of two genes of pluripotency (Oct4 and Rex1) in order to evaluate if the overexpression of each microRNAs by itself could alter the pluripotency of mESCs. In figure 23, mean expression data are presented showing no statistical differences between the four cell lines (mESC-D3, mESC-empty, mESC-miR-1, and mESC-miR-423) for Oct4, while we found a slight but significant up-regulation of Rex1 in the three engineered cell lines compared to the control line.

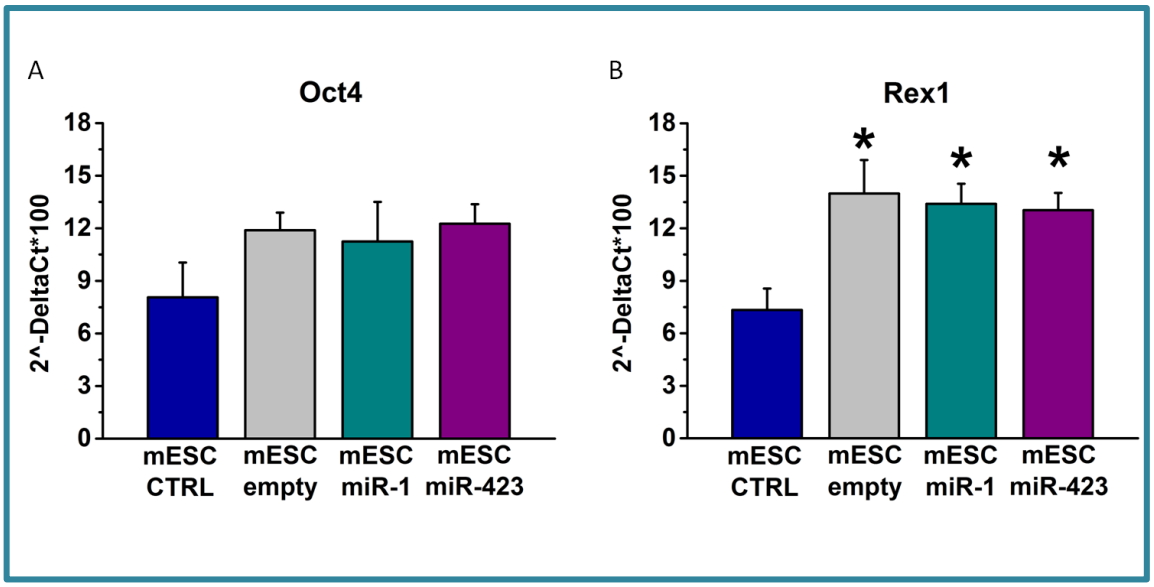

Fig 23: mean expression of Oct4 mRNA **(A)** and Rex1 mRNA **(B)** in mESC-D3 (blue, n=3), in mESC-empty (grey, n=3), in mESC-miR-1 (green, n=4), and in mESC-miR-423 (purple, n=4) * p<0,05 (ANOVA, Fisher test).

5.3 Differentiation of mESC into sinoatrial-like cardiomyocytes with pacemaker phenotype

We evaluated the ability of these cells to correctly differentiate into cardiomyocytes using the Hanging Drops technique, a well-established protocol that allows the formation of Embryoid Bodies (EBs), small compact cell aggregates that resemble early stages of the embryo development (*Maltsev et al., 1994*). After at least 7 days of differentiation, little regions of EBs start to beat spontaneously and the beating activity was monitored for the next 7 days; in the table 9 the percentage of beating EBs of the three mESCs lines is shown. These results suggest the effective differentiation of cells into cardiomyocytes and that the overexpression of miR-1 and miR423 did not alter the capacity of mESCs to properly differentiate into beating cardiomyocytes. These results are in accordance with previously published data (*Barbuti et al., 2009*).

	mESC empty	mESC-miR-1	mESC-miR-423
7+1	85.2±5.4% (n=8)	87.6±3.2% (n=8)	92.0±5.1% (n=6)
7+2	85.5±5.2% (n=8)	93.4±1.7% (n=8)	96.2±3.3% (n=6)
7+3	78.6±7.0% (n=5)	77.6±17.3% (n=5)	93.7±5.4% (n=3)
7+4	78.8±6.3% (n=5)	96.6±2.2% (n=5)	98.7±0.7% (n=3)
7+5	98.0±2.0% (n=3)	97.3±0.7% (n=3)	98.7±0.7% (n=3)
7+6	98.0±2.0% (n=3)	91.7±9.3% (n=3)	94.0±2.1% (n=3)
7+7	87.7±5.9% (n=8)	94.8±2.0% (n=8)	93.7±3.4% (n=6)

Tab. 9: mean percentage of beating EBs at different days of differentiation (from 8 to 14), obtained from mESC-empty, mESC-miR-1, and mESC-miR-423.

In order to specifically isolate sinoatrial-like cells from EBs at day 8 of differentiation, we selected cells positive for the CD166 marker, since this protein is known to identify SAN progenitors from differentiating mESCs (*Scavone et al., 2013*).

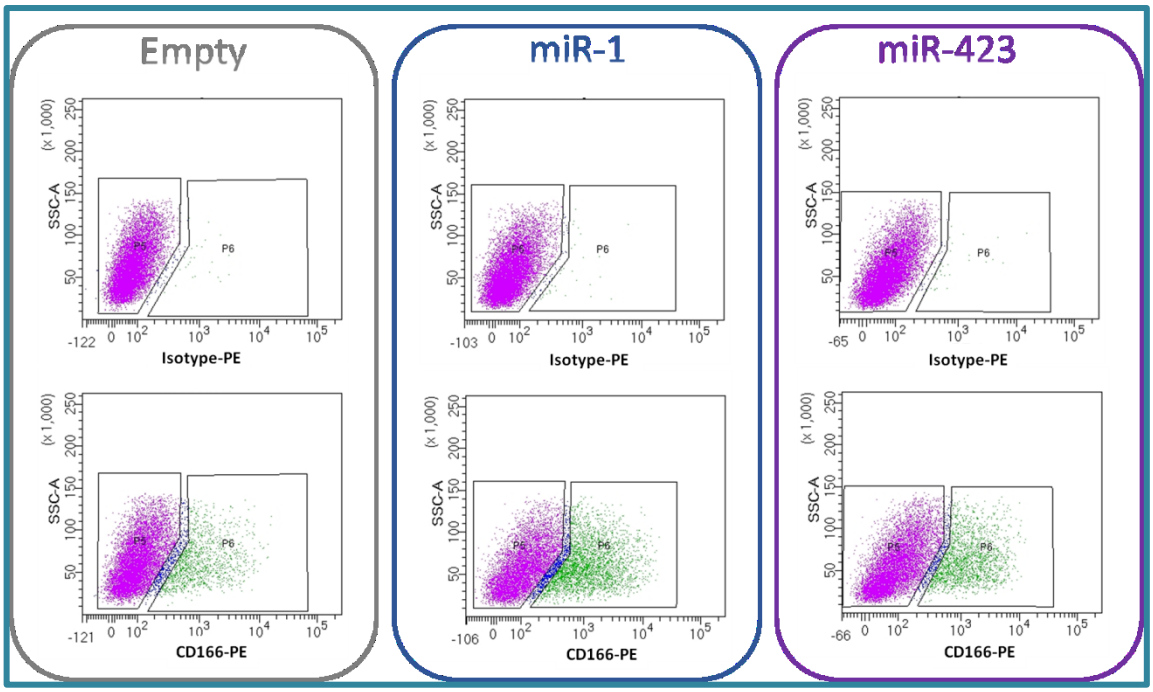

Fig 24: representative dot plot of CD166+ cells analysis at day 8 of differentiation from EBs obtained from mESC-empty, mESC-miR-1, and mESC-miR-423, the negative population is set for each line labeling cells with the proper isotype.

CD166+ cells have been sorted and re-aggregated by gravity for 24h in low-adhesion culture dishes in differentiating medium, and subsequently plated at high density (10^5 cells/mm^2) in silicon inserts to allow the formation of a compact beating layer. Once plated, CD166+ cells formed, as expected, a compact aggregate of spontaneously beating sinoatrial-like cells. The bar graph of fig. 25, shows that the percentage of CD166 positive cells is statistically higher in mESC-miR-1 and mESC-miR-423, than in the control cell line (25.20±2.32 in CD166+-miR-1 vs 11.09±1.09 in CD166+-empty vs 18.56±1.36 CD166+-miR-423).

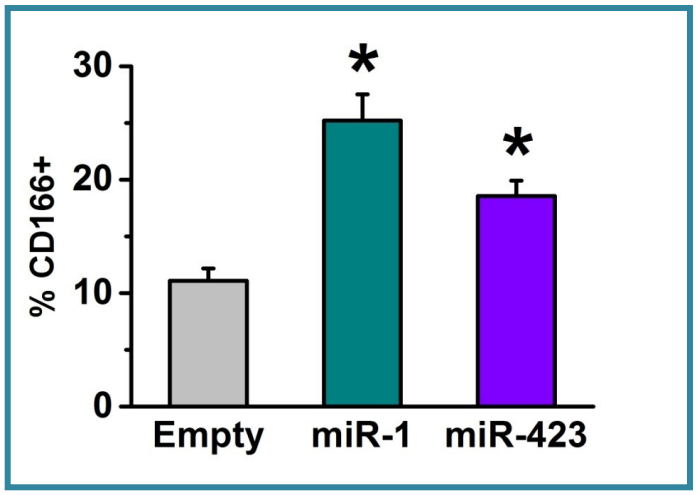

Fig 25: mean percentage of CD166+ cells in EBs obtained from the differentiation of mESC-empty (grey, n=30), mESC-miR-1 (green, n=26), and mESC-miR-423 (purple, n=9) at day 8 of differentiation. * p<0,05 (ANOVA, Fisher test).

After the sorting selection, we compared the α-Actinin expression in CD166+ and in CD166- cells, using quantitative real-time PCR: as expected, the CD166+ cells express α-Actinin at higher levels than CD166- cells (Fig. 26 and Tab. 10).

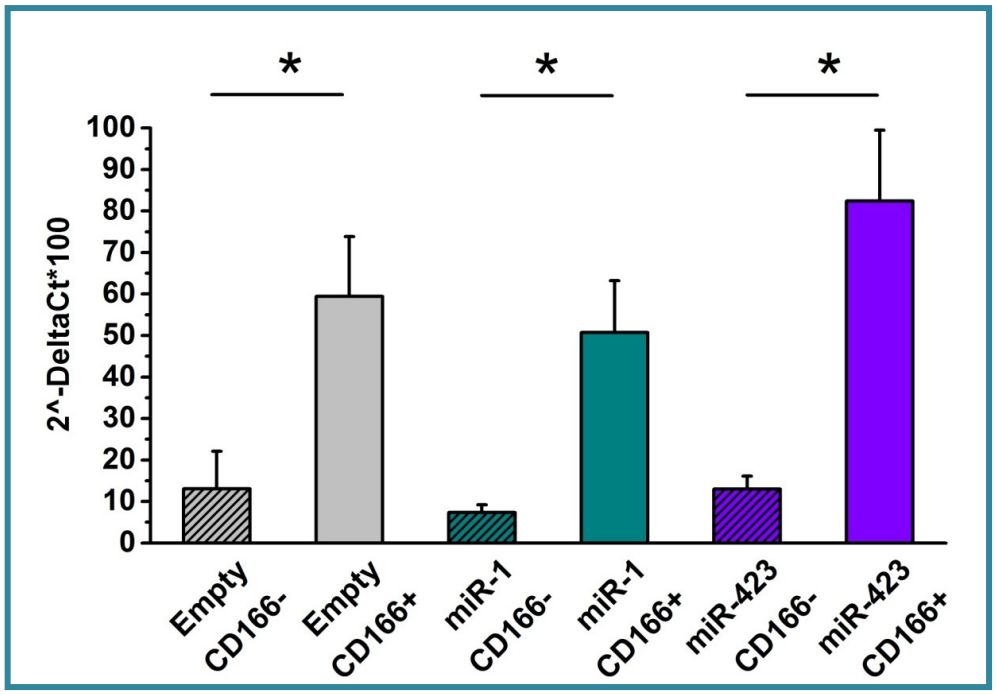

Fig 26: mean expression of α-Actinin mRNA in Empty-CD166- (dashed grey, n=10), Empty-CD166+ (grey, n=10), miR1-CD166- (dashed green, n=9), miR1-CD166+ (green, n=9), miR423-CD166- (dashed purple, n=7), and miR423-CD166+ (purple, n=7). No differences between all CD166- cell lines and no differences between all CD166+ cell lines (ANOVA, Fisher test). * p<0,05 (t-test between CD166+ and CD166- of all cell lines).

	CD166-	CD166+
Empty	13.10±9.02 (n=10)	59.41±14.42 (n=10)
miR-1	7.35±1.84 (n=9)	50.76±12.46 (n=9)
miR-423	13.01±3.11 (n=7)	82.42±17.06 (n=7)

Tab. 10: mean expression of α-Actinin mRNA in CD166+ and CD166- cells of all three cell lines. Data are expressed as mean±SEM.

We further evaluated the expression levels of some genes expressed and involved in the earliest stages of SAN differentiation (Shox2 and Tbx18), finding no differences in miR-1-CD166+, miR-423-CD166+, empty-CD166+, and SAN except for the Tbx18 level in CD166+-miR-1, that was statistically higher than in the other samples (Fig. 27; Tab. 11). These results support not only the idea that miR-1 is involved in the mesoderm and muscle-line differentiation, but also that the overexpression of the different plasmids does not affect the capacity of mESC to properly differentiate in sinoatrial-like cells.

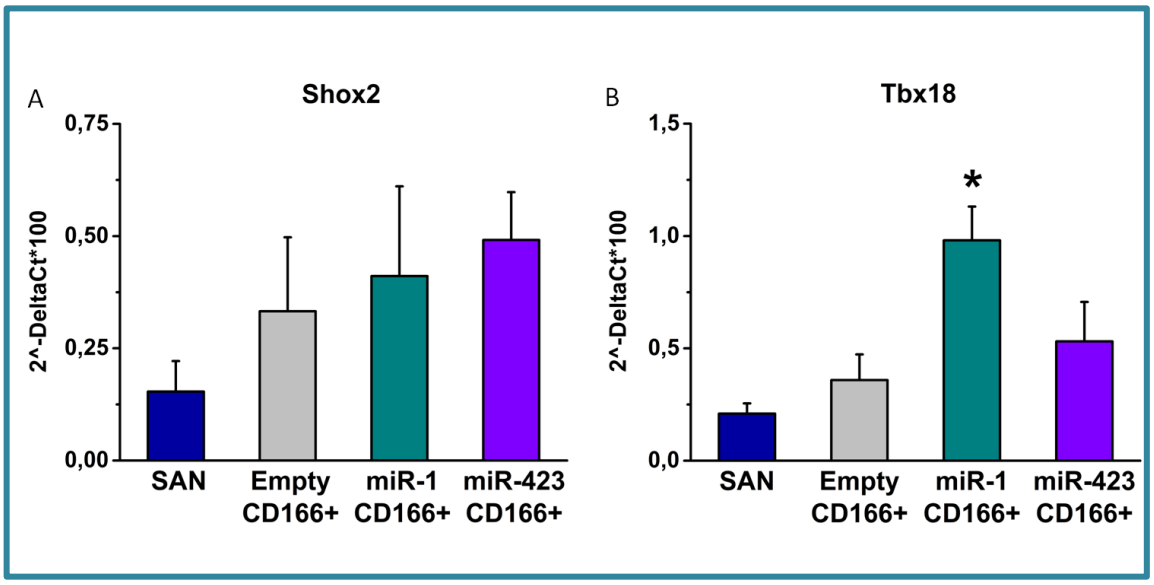

Fig 27: **(A)** mean expression level of Shox2 mRNA in mouse SAN (blue, n=5) and in CD166+ of empty line (grey, n=9), of miR-1 line (green, n=15), and of miR-423 (purple, n=6). **(B)** Mean expression level of Tbx18 mRNA in mouse SAN (blue, n=5) and in CD166+ of empty line (grey, n=10), of miR-1 line (green, n=14), and of miR-423 (purple, n=7).* p<0,05 (ANOVA, Fisher test).

	Shox2	Tbx18
SAN	0.15±0.07 (n=5)	0.21±0.05 (n=5)
Empty CD166+	0.33±0.17 (n=9)	0.36±0.11 (n=10)
miR-1 CD166+	0.41±0.20 (n=15)	0.98±0.15 (n=14)
miR-423 CD166+	0.49±0.26 (n=6)	0.53±0.18 (n=7)

Tab. 11: mean expression of Shox2 and Tbx18 mRNAs in mouse SAN and CD166+ of empty, miR-1 and miR-423 cell lines. Data are expressed as mean±SEM.

Knowing that the expression of the I_f current, and in particular of the HCN4 isoform, is a necessary condition to properly identify SAN cells, and since miR-1 and miR-423 bind to HCN4 3'UTR, we also evaluated the expression levels of HCN4 in the sinoatrial-like cells (CD166+ cells) obtained from the various lines (mESC-empty, mESC-miR-1, and mESC-miR-423), using quantitative real-time PCR. The bar graph (Fig. 28) shows no statistical differences between HCN4 levels in empty-CD166+, miR-1-CD166+, and miR-423-CD166+ (empty-CD166+ 3.00±0.41 n=15; miR-1-CD166+ 3.08±0.40 n=14; miR-423-CD166+ 3.91±0.98 n=7).

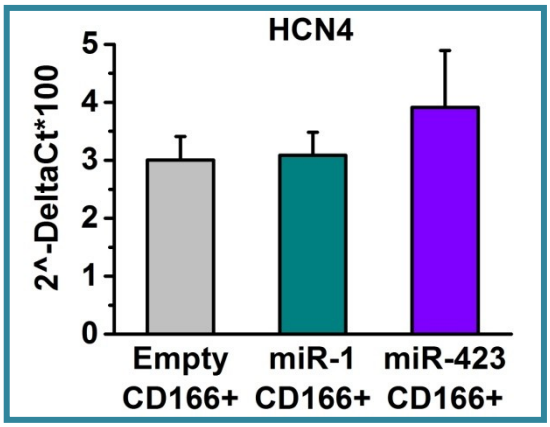

Fig 28: mean expression of HCN4 mRNA in empty-CD166+ (grey, n=15), miR-1-CD166+ (green, n=14), and miR-423 (purple, n=7) * p<0,05 (ANOVA, Fisher test).

Furthermore, we analyzed the expression of HCN4 and α-actinin at the protein level in CD166+ cells of all three cell lines. Representative immunofluorescence images are shown in Figure 29. We did not observe any strong difference in the expression pattern. These results further confirm that the CD166+ cells isolated from EBs at day 8 of differentiation from mESC-empty, mESC-miR-1, and mESC-miR423 are cardiomyocytes with sinoatrial properties.

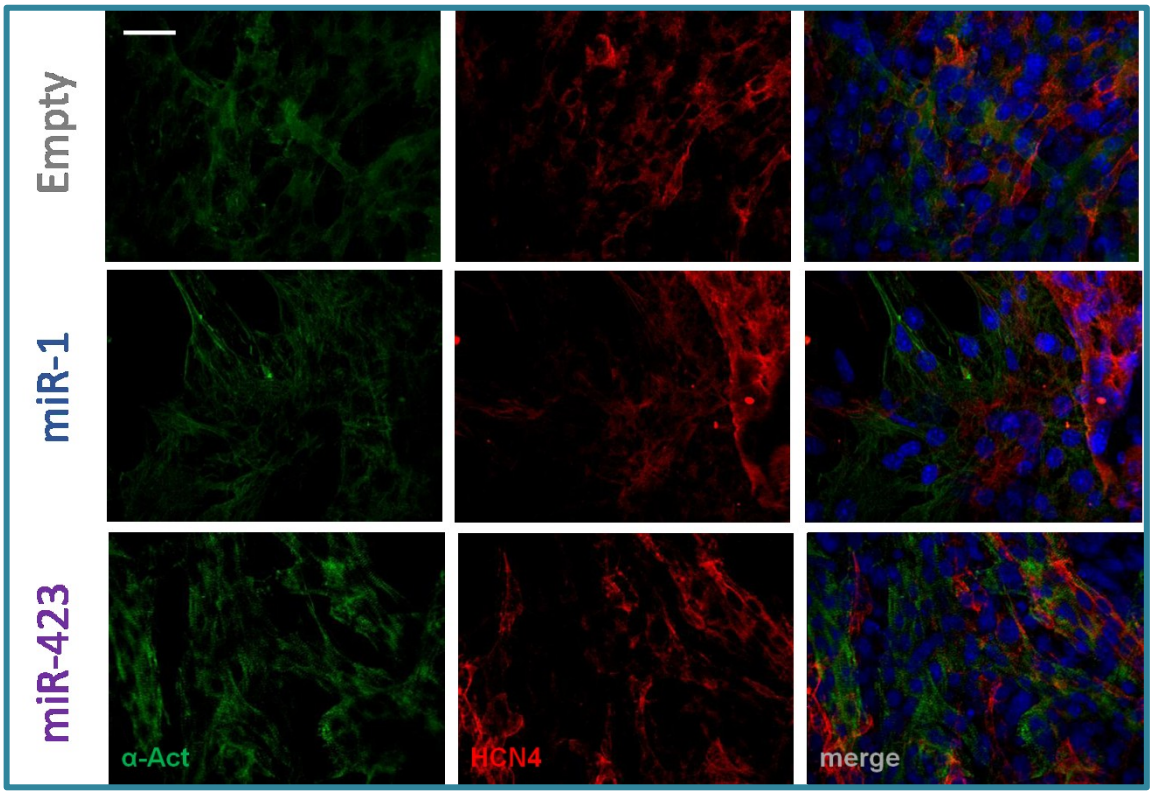

Fig 29: confocal images of CD166-selected cells for empty, miR-1, and miR-423 lines: cells were stained with either the cardiac proteins α-Actinin (green) and HCN4 (red). Nuclei were stained with 4',6-diamidino-2-phenylindole (DAPI). Calibration Bar 35μm.

5.4 Electrophysiological analysis on sinoatrial-like cells

We have then investigated the functional properties of sinoatrial-like cells by patch-clamp analysis, in the whole-cell configuration. First, we performed current-clamp experiments in order to evaluate the spontaneous beating rate of the CD166+ layer. On average, miR-1-CD166+ cells showed a 38% reduction of the rate compared to the empty-CD166+ cells. No differences were instead found between miR-423-

CD166+ and empty-CD166+ cells (miR-1-CD166+ 1.37±0.08 Hz n=10; miR-423-CD166+ 2.36±0.30 Hz n=7; empty-CD166+ 2.22±0.22 Hz n=7) (Fig. 30).

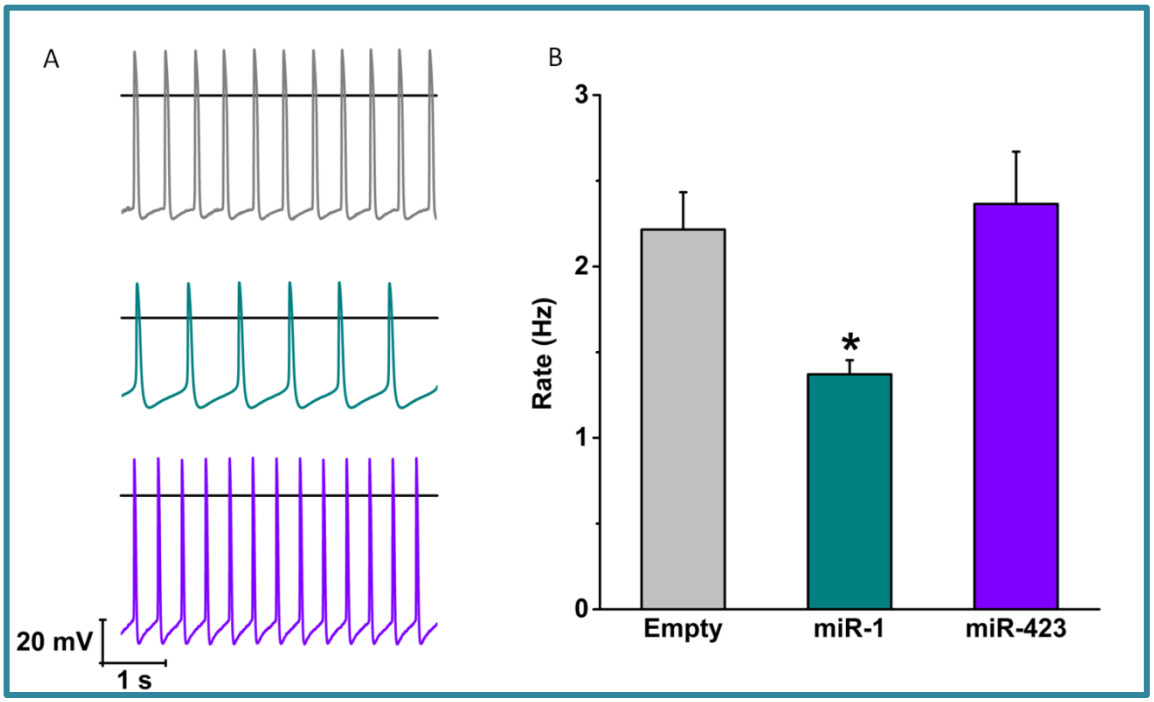

Fig. 30: **(A)** representative traces of action potentials recorded from CD166+ cells of empty line (grey), of miR-1 line (green), and of miR-423 line (purple). **(B)** Mean action potential rate of CD166+ cells of empty line (grey), of miR-1 line (green), and of miR-423 line (purple). * p<0,05 (ANOVA, Fisher test).

These data suggest that the miR-1 overexpression leads to a reduction of beating rate in sinoatrial-like cells, and we can assume that this slowdown of the rhythm is due to a reduction of I_f current. In order to verify this hypothesis, we carried out electrophysiological recording in voltage-clamp configuration on single cells dissociated from the compact beating layer of miR-1-CD166+ and empty-CD166+. The steady state current amplitude was measured in the range of potentials from -35mV to -125mV with steps of 10mV, and these values were normalized to cell capacitance to obtain current densities. As evident from the representative traces of I_f current and from the mean current density plot, the funny current results statistically reduced in CD166+ overexpressing miR-1, whit a reduction of 50%. While there are no differences in the voltage dependence of the channels as evident from the activation curve (Fig. 31).

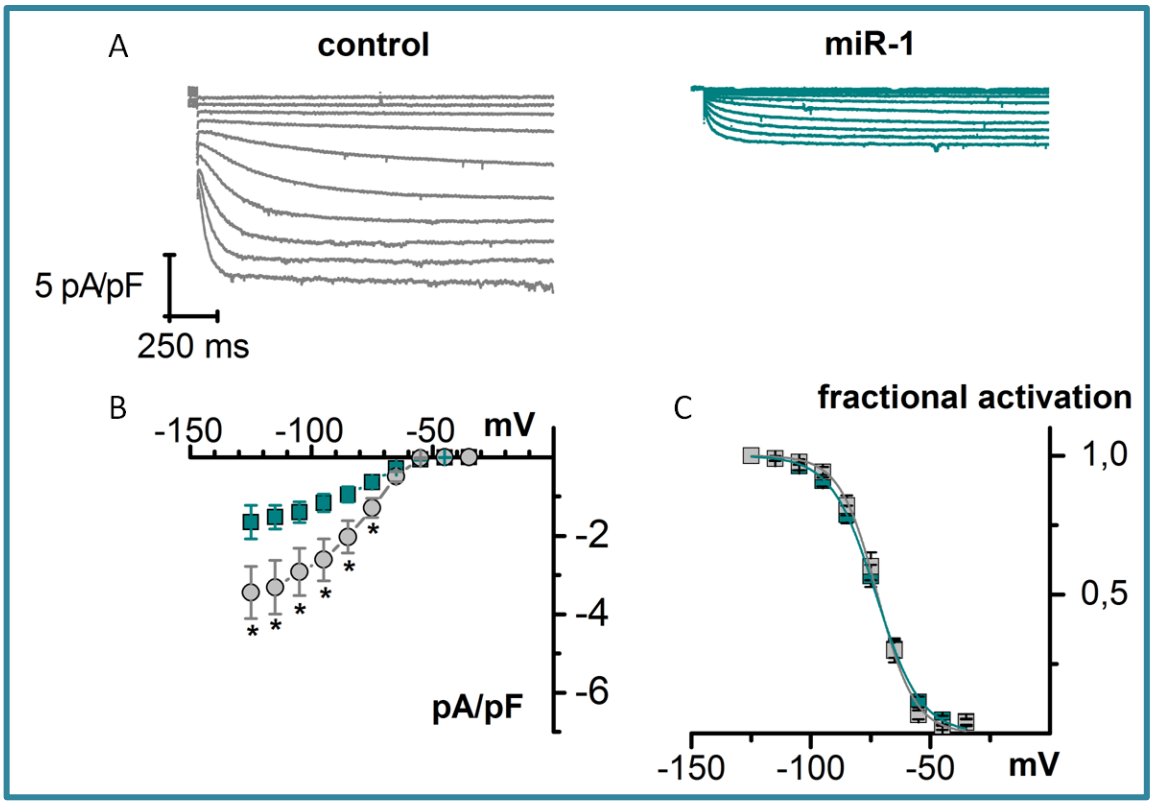

Fig. 31: **(A)** representative traces of I_f current recorded from CD166+ cells of empty line (grey) and miR-1 line (green). **(B)** Plot of current density of CD166+ cells of empty line (grey) and miR-1 line (green). **(C)** Activation curve of funny current of CD166+ cells of empty line (grey) and miR-1 line (green). * p<0,05 (t-test).

	$V_{1/2}$	Slope
Empty CD166+	-72.69±1.55 (n=19)	6.77±0.53 (n=19)
miR-1 CD166+	-73.13±1.32 (n=30)	8.03±0.38 (n=30)

Tab. 12: mean $V_{1/2}$ and slope of empty-CD166+ and miR-1-CD166+. Data are expressed as mean±SEM.

5.5 Expression of miR-1 and miR-423 in CD166+ cells

We also decided to evaluate the expression levels of miR-1 and miR-423 in CD166+ cells, and as visible in the bar graph in figure 32, miR-1 results up-regulated in CD166+ cells, isolated from EBs differentiated from mESC-miR-1 compared to CD166+ cells isolated from the EBs obtained from the control line (mESC-empty) (mESC-miR-1 46.86±17.58, n=12; mESC-empty 3.01±1.72, n=10). While, surprisingly, we did not find any difference in the expression level of miR-423 in CD166+ positive cells isolated from EBs differentiated from mESC overexpressing miR-423 and the control (mESC-miR-423 1.24±0.85, n=7; mESC-empty 0.92±0.40, n=9) (Fig. 32).

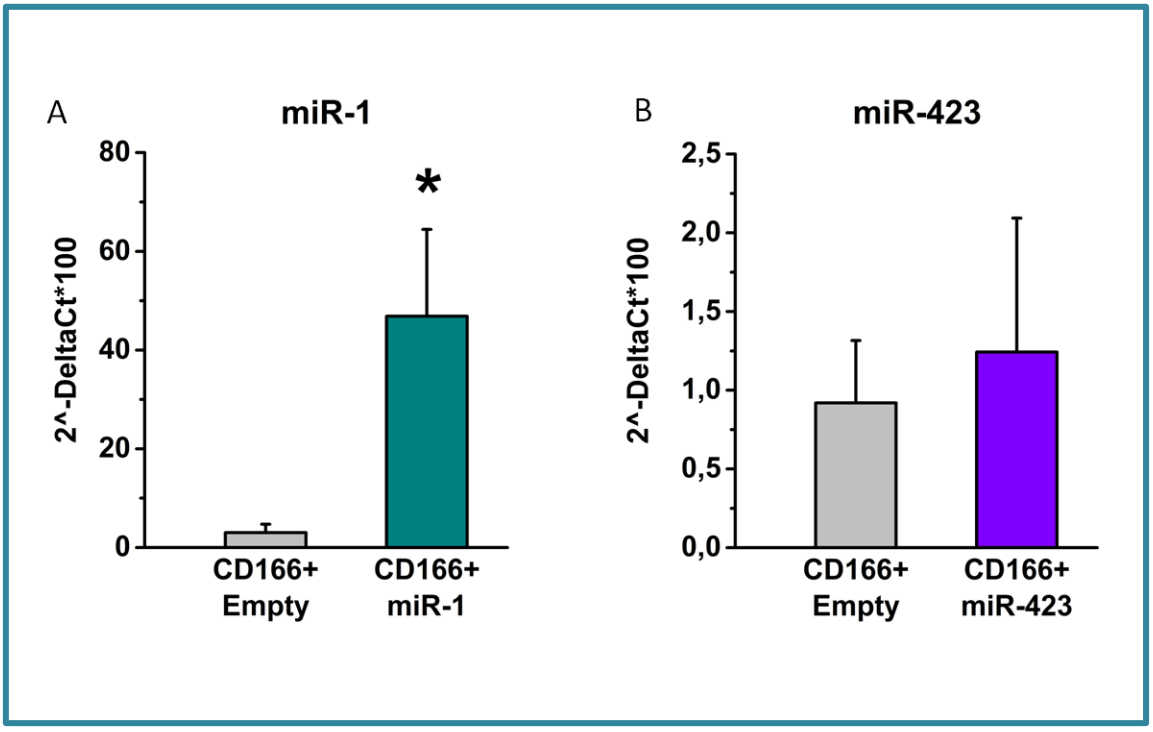

Fig. 32: **(A)** mean expression of miR-1 empty-CD166+ cells (grey, n=10) and miR-1-CD166+ (green, n=12). **(B)** Mean expression of miR-423 empty-CD166+ cells (grey, n=9) and miR-423-CD166+ (purple, n=7). Note the difference in the y scale. * p<0,05 (t-test).

5.6 Electrophysiological analysis of rat ventricular cardiomyocytes overexpressing miR423

Since we found no differences in the expression levels of miR-423 between miR-423-CD166+ and empty-CD166+, we decided to evaluate if the similar beating rate of these cells is due the insufficiently high expression of miR-423 or because miR-423 does not affect the electrical properties of sinoatrial-like cells. To do this, we transiently transfect neonatal rat ventricular cardiomyocytes (NRVCs), that display spontaneous activity, with the miR-423 plasmid and with the control empty plasmid. After 48 hours of transfection, we recorded spontaneous action potentials (APs) from little aggregates of NRVCs, displaying green fluorescence. We did not find differences in the mean beating rate of NRVC-empty (1.37±0.51Hz, n=3) and NRV-miR-423 (1.57±0.30Hz, n=10) (Fig. 33).

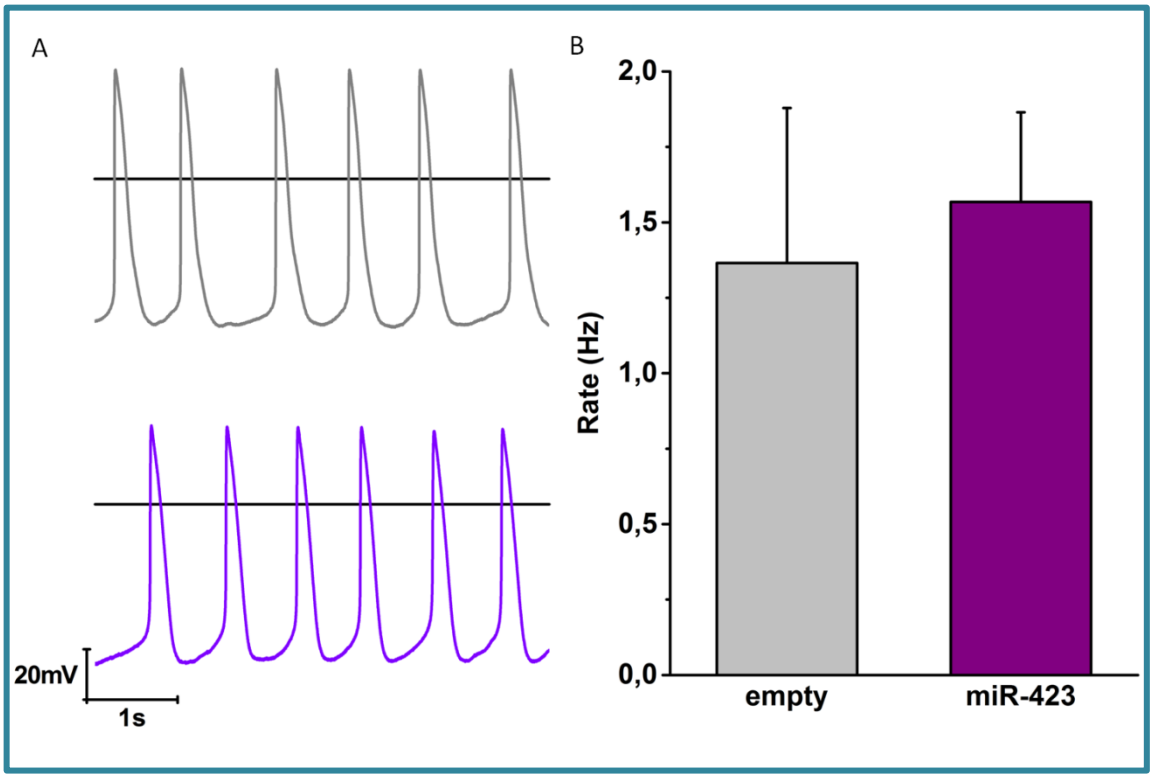

Fig. 33: representative traces **(A)** and mean **(B)** of action potentials recorded from NRVC transfected with the empty plasmid (grey) or overexpressing miR-423 (purple).

6. Discussion

It is well known that regular physical activity confers a plethora of health benefits. Endurance training requires electrical, structural, and functional adaptation of the heart in order to sustain the increased metabolic need and thus the cardiac output. This remodeling is referred as “Athletes Heart”. One of the most common adaptation in endurance athletes is deep bradycardia, a heart rhythm lower than 60 beats/min, with episodes of 30 beats/min. Endurance training bradycardia is commonly associated with an increased vagal tone, but recently it was demonstrated that in trained animals (rats and mice) it is due to an intrinsic modification of the pacemaker property of the heart, and in particular to a reduction of the funny current. This current is fundamental in the early diastolic depolarization phase of the action potential, and so for the setting of the heart rhythm (*D’Souza et al., 2014*). Recently, microRNAs (miRNAs) were discovered as novel modulators of pathologic and physiologic remodeling of the heart. D’Souza and co-workers demonstrated an up-regulation of miR-1, one of the main muscle-specific microRNAs, in the SAN of trained mice, and moreover they recently demonstrated that miR-423 is also up-regulated in SAN of trained mice and that both miRNAs directly binds the 3’UTR of the HCN4 channels, the main molecular component of the I_f current in SAN cells (*D’Souza et al., 2014*).
We thus decided to study the role of these microRNAs on SAN function. SAN myocytes are difficult to isolate, the yield of cells is usually poor and they cannot be kept in culture for more than a couple of days. Only recently it was demonstrated, by St. Clair and collaborators, that sinoatrial myocytes from adult mice can be kept in culture for up to one week, that it is possible to infect them using adenovirus, but it is not possible to transiently transfect them, making very challenging working with them. Moreover, a huge problem is the small size of mice SAN and consequently the very small number of cells that it is possible to isolate that rapidly decreases in culture. St. Clair and colleagues also underlined the necessity to keep the BDM (2,3-butanedione monoxime), a reversible contraction inhibitor, in the culture medium, a procedure that caused different side effects, such as the inhibition of different cardiac transcription factors and some ion currents (sodium and calcium) (*St. Clair et al., 2015*). To overcame these limitations, we decided to study the role of these two

microRNAs in sinoatrial-like cells obtained from mESCs (*Scavone et al., 2013*) overexpressing miR-1 and miR-423.

Since during cell electroporation the plasmid could be integrated casually into the genome, it is possible that the insertion in an important region could alter the fundamental properties of cells. For this reason, we decided to evaluate if the pluripotency of mESC is conserved in the various clones. Besides maintaining an elevated proliferative potential and a correct morphology (data not shown), analyzing the expression levels of Oct4 and Rex1, we demonstrated that all the three cell lines obtained maintain high expression levels of these two markers indicating that they have their pluripotency characteristics unaltered. In the same way it is possible that either the random integration of the plasmid or the overexpression or the miR by itself can interfere with the normal differentiation pathways. Thus, we also evaluated the capacity of our cell lines to properly differentiate into cardiomyocytes and we found that, using the Hanging Drop technique, they are able to form EBs that display spontaneous beating activity at day 7 of differentiation, according to what previously demonstrated in our laboratory using various mESC lines (*Barbuti et al., 2009; Scavone et al., 2013*). Knowing that microRNAs have diverse effects in different cells and conditions, in this way we also demonstrated that the miR-1 and miR-423 overexpression do not affect the pluripotency of mESCs and neither their capacity of properly differentiate into cardiomyocytes, as previously showed by Ivey and collaborators for miR-1 (*Ivey et al., 2008*).

The CD166+ cells obtained from all the three cell lines show comparable characteristics from those obtained by Scavone and coworkers, indeed CD166+ cells show higher level of α-Actinin than CD166- and they expressed α-Actinin and HCN4 at protein level with an expression pattern comparable with of those of control cells (Fig. 34) (Scavone et al., 2013).

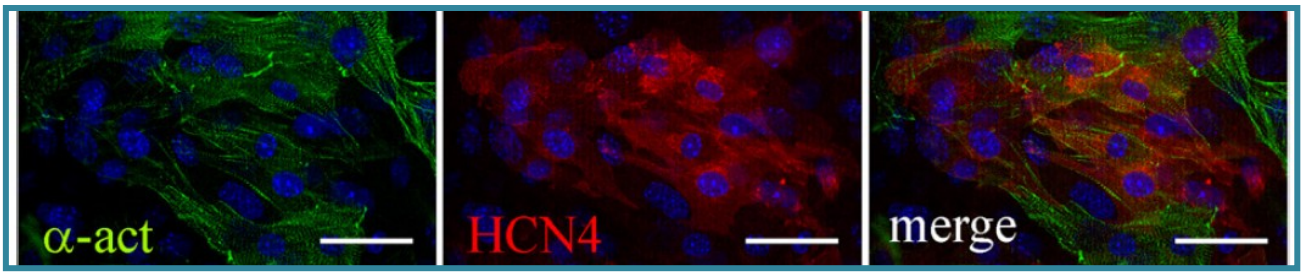

Fig. 34: confocal images of CD166+ cells labelled with α-Actinin (α-act, green) and HCN4 (red); nuclei were stained with DAPI. Calibration bars, 50 μm (modified from *Scavone et al., 2013*).

In order to further confirm the proper differentiation of mESCs into cardiomyocytes with a sinoatrial-like phenotype we evaluated the expression level of Shox2 and Tbx18, two genes involved in the earliest stage of SAN development (*Barbuti and Robinson, 2015*). We found that CD166+ cells of all three cell lines express Shox2 and Tbx18, at comparable levels with SAN of adult mice and in accordance with what previously found (*Scavone et al., 2013*). It is possible to observe only an up-regulation of Tbx18 in miR-1-CD166+ in comparison to the control line. This result could be due to the fact that miR-1 is known to be involved in mesodermal and cardiac differentiation (*Ivey et al., 2008).*

The percentage of CD166 positive cells, the sinoatrial-like cells, at day 8 of differentiation in EBs differentiated from mESC-miR-1 is statistically higher than those in EBs obtained from the control cell line, and this is in agreement with literature data, indeed it was demonstrated that miR-1 has a double function: first, it induces the mesodermal lineages, and then supports the muscle-line differentiation (*Ivey et al., 2008*). From our results we can say that mESC-derived sinoatrial-like cells can be generated from mESC lines overexpressing the miR of interest and can thus be used as a cellular model to study the effects of miRNAs on pacemaking mechanisms.

D'Souza and coworkers demonstrated that trained bradycardia is due to an intrinsic reduction of the beating rate of SAN cells, and to a reduction of the funny current, rather than a reduction of the vagal tone on the heart, but the molecular mechanism at the bases of this process is not completely understood. They also demonstrated that miR-1 is up-regulated in SAN of trained mice and hypothesized that these microRNAs could be involved in the mechanism at the basis of beating rate reduction of SAN of trained mice. Here we found that the miR-1-CD166+ cells display a

reduction of the beating rate and of the funny current, and so we can conclude that the overexpression of miR-1 is involved in the setting of the heart rhythm and in particular its overexpression induces a reduction of the action potential firing rate, modulating the I_f current of sinoatrial-like cells. These data are in accordance with the reduction of heart rate of trained mice and with the reduction of the beating rate and of the funny current of SAN cells isolated from trained mice founded by D'Souza and coworkers (*D'Souza et al., 2014*). So it is possible to speculate that the trained induced bradycardia may be due to a reduction of beating rate of SAN cells due to a reduction of the funny current mediated by an increase of miR-1 expression.

We find no differences on the HCN4 mRNA levels in miR-1-CD166+ and in empty-CD166+ cells, suggesting that the binding between miR-1 and HCN4 mRNA lead to a translational repression, rather than a mRNA degradation. This result is in contrast with the reduction of the HCN4 mRNA found by D'Souza and collaborators in SAN cells of trained mice and rats. This discrepancy could be explained by the different models used, indeed we studied only the overexpression of miR-1 in sinoatrial-like cells, while D'Souza studied a more complex model of trained mice, where the reduction of the HCN4 transcript could be due to other mechanisms like, for example, the modulation by other miRNAs.

The activation curves of the I_f current obtained during the patch-clamp experiments, and recorded from the miR-1-CD166+ and empty-CD166+ are similar and, suggesting that the reduction of the funny current is due to a direct action of miR-1 on HCN4 mRNA in accordance with the results of our collaborators of Manchester that found a direct bind between miR-1 and the 3'UTR of HCN4 mRNA.

Regarding miR-423, little it is known in the literature. At present, it is known that miR-423 is associated with heart failure, unstable angina pectoris, and dilated cardiomyopathy; but it is not associated with myocardial infarction (*Tijsen et al., 2010; Bauters et al., 2013; Miyamoto et al., 2015).* These data suggest that miR-423 is altered in different cardiac pathology, but actually is not associated with rhythm disturbances. Our collaborators found an up-regulation of miR-423 in SAN of trained mice and, using the luciferase report assay, they demonstrated that it directly binds the 3'UTR of HCN4 mRNA. We thus studied the overexpression of miR-423 in sinoatrial-like cells, finding no differences in the AP firing rate compared with the control.

When we analyzed the expression levels of miR-423 in miR-423-CD166+ and in control cells, we found no differences, while this overexpression, although limited, was present in mESC-miR-423 cells. We currently don't know why the miR-1 overexpression persists after the differentiation of mESC, while the same result is not true for miR-423, but we supposed that this could be due to its limited overexpression (~3 times) respect the higher overexpression of miR-1 (~$2x10^4$) in mESCs after electroporation. Consequently, these results lead us to suppose that the electrophysiological data could be vitiated by the lack of miR-423 overexpression in sinoatrial-like cells. For this reason, we decided to study the effects of miR-423 overexpression in another well-established excitable model, already used in our laboratory to study the functional role of some microRNAs in a cardiac context. Indeed, we transiently transfected neonatal rat ventricular cardiomyocytes with the miR-423 and control plasmids, and again we found no differences in the AP firing rate. These data suggest that, despite miR-423 is altered in SAN of trained mice and it directly binds the 3'UTR of HCN4 mRNA in the luciferase assay, it is not probably involved in the regulation of beating rate of trained mice. The discrepancies in the results are explainable by the fact that it is known from the literature that the same miRNA could have different effects in different cellular contexts, and it is increasingly clear that the results *in vitro* with the luciferase assay are not completely truthful and they must be confirmed with other experiments. However, it would be desirable to evaluate the expression level of miR-423 in rat ventricular cardiomyocytes transfected with the two plasmid before ruling out the role of miR-423; indeed it would be better to check that the lack of effect is not duo to a possible low expression of the plasmid also in this cellular model.

All these data together lead us to conclude that miR-1 and miR-423 are up-regulated in SAN cells of trained mice, and they directly bind the 3'UTR of HCN4 channels. So it is possible to speculate that miR-1 is one of the microRNAs involved in the trained-induced bradycardia in mice. These results provide us another important conclusion: in particular we demonstrated that this cellular model is exploitable to study the role of different microRNAs in a sinoatrial context. Knowing that microRNAs could have different effects in different cellular contexts, it is important to study the role of a microRNAs in the right and specific cellular model (*Bartel, 2009*). Since SAN cells are limited in number and not accessible, in particular in humans, for biological studies, it is important to find other ways to obtain this kind of cells to study the role of miRNAs.

Very recently, Protze and coworkers demonstrated that it is possible to isolate human sinoatrial-like cells from human pluripotent stem cells, and consequently it is possible to speculate that the combination of our technique and the differentiation and isolation protocol of Protze would make possible to study the role of microRNAs in human sinoatrial-like cells to better understand the mechanism at the basis of human heart rhythm (*Protze et al., 2016*).

7. References

Altomare C., Bucchi A., Camatini E., Baruscotti M., Viscomi C., Moroni A., DiFrancesco D. (2001) Integrated allosteric model of voltage gating of HCN channels. *J Gen Physiol;117(6):519-32.*

Baldesberger S., Bauersfeld U., Candinas R., Seifert B., Zuber M., Ritter M., Jenni R., Oechslin E., Luthi P., Scharf C., Marti B., and Attenhofer Jost C. H. (2008) Sinus node disease and arrhythmias in the longterm follow-up of former professional cyclists. *European Heart Journal, 71–78*

Barbuti A, Terragni B, Brioschi C, DiFrancesco D. (2007) Localization of f-channels to caveolae mediates specific beta2-adrenergic receptor modulation of rate in sinoatrial myocytes. *J Mol Cell Cardiol. ;42(1):71-8.*

Barbuti A, Crespi A, Capilupo D, Mazzocchi N, Baruscotti M, DiFrancesco D. (2009) Molecular composition and functional properties of f-channels in murine embryonic stem cell-derived pacemaker cells. *J Mol Cell Cardiol. 46:343–351.*

Barbuti A and Robinson R.B. (2015) Stem Cell–Derived Nodal-Like Cardiomyocytes as a Novel Pharmacologic Tool: Insights from Sinoatrial Node Development and Function. *Pharmacological Reviews*

Bartel D. P. (2009) MicroRNA: target recognition and regulatory function. *Cell 136, 215–233*

Bauters C., Kumarswamy R., Holzmann A., Bretthauer J.,Anker S.D., Pinet F., Thum T; (2013) Circulating miR-133a and miR-423-5p fail as biomarkers for left ventricular remodeling after myocardial infarction. *International Journal of Cardiology 168 1837–1840*

Benito B, Gay-Jordi G, Serrano-Mollar A, Guasch E, Shi Y, Tardif J-C, Brugada J, Nattel S, Mont L. (2011) Cardiac arrhythmogenic remodeling in a rat model of long-term intensive exercise training. *Circulation;123:13–22.*

Brioschi C, Micheloni S, Tellez JO, Pisoni G, Longhi R, Moroni P, Billeter R, Barbuti A, Dobrzynski H, Boyett MR, DiFrancesco D, Baruscotti M. (2009) Distribution of the pacemaker HCN4 channel mRNA and protein in the rabbit sinoatrial node. *J Mol Cell Cardiol.47(2):221- 7.*

Brown HF, DiFrancesco D, Noble SJ (1979) How does adrenaline accelerate the heart? *Nature; 280:235-236*

Brown HF, DiFrancesco D (1980) Voltage clamp investigations of membrane currents underlying pacemaker activity in rabbit sino-atrial node. *J Physiol (Lond); 308:331-351.*

Callis T.E. and Wang D. (2008) taking microRNAs to heart trends in molecular medicine. *Cell press. Pages 254–260*

Cerbai E, Mugelli A (2006) I(f) in non-pacemaker cells: Role and pharmacological implications. *Pharmacol Res;53:416-423*

Coote J. H. and White M. J. (2015) CrossTalk proposal: Bradycardia in the trained athlete is attributable to high vagal tone. *J Physiol 593.8 pp 1745–1747*

De Miguel MP, Fuentes-Julián S, Alcaina Y. (2010) Pluripotent stem cells: origin, maintenance and induction. *Stem Cell Rev. 6(4):633-49.*

DiFrancesco D, Ojeda C (1980) Properties of the current if in the sinoatrial node of the rabbit compared with those of the current iK2 in Purkinje fibres. *J Physiol (Lond); 308:353-367*

DiFrancesco D (1981) a A study of the ionic nature of the pace-maker current in calf Purkinje fibres. *J Physiol (Lond); 314:377-393*

DiFrancesco D (1981) b A new interpretation of the pace-maker current in calf Purkinje fibres. *J Physiol (Lond); 314:359-376*

DiFrancesco D, Ferroni A, Mazzanti M and Tromba C (1986) a Properties of the hyperpolarizing-activated current (I_f) in cells isolated from the rabbit sino-atrial node. *The Journal of Physiology*

DiFrancesco D. (1986) b Characterization of single pacemaker channels in cardiac sino-atrial node cells. *Nature; 324:470-473*

DiFrancesco D, Tortora P (1991). Direct activation of cardiac pacemaker channels by intracellular cyclic AMP. *Nature 351: 145–147*

DiFrancesco D. and Borer JS. (2007) The Funny current. Cellular basis for the control of heart rate. *Drugs 67 (suppl 2)15-24.*

D'Souza A, Bucchi A, Johnsen AB, Logantha SJRJ, Monfredi O, Yanni J, Prehar S, Hardt G, Cartwright E,Wisloff U, Dobryznski H, DiFrancesco D, Morris GM & Boyett MR (2014). Exercise training reduces the resting heart rate via downregulation of the funny channel HCN4. *Nat Commun 5, 3775.*

Duan L., Xiong X., Liu Y., Wang J. (2014) miRNA-1: functional roles and dysregulation in heart disease. *Mol Biosyst.*

Espinoza-Lewis RA, Yu L, He F, Liu H, Tang R, Shi J, Sun X, Martin JF, Wang D, Yang J, et al. (2009) Shox2 is essential for the differentiation of cardiac pacemaker cells by repressing Nkx2-5. *Dev Biol 327:376–385.*

Friedman R. C., Farh K. K., Burge C. B. and Bartel D. P. (2009) Most mammalian mRNAs are conserved targets of microRNAs. *Genome Res. 19, 92–105.*

Gassanov N, Er F, Zagidullin N, and Hoppe UC (2004) Endothelin induces differentiation of ANP-EGFP expressing embryonic stem cells towards a pacemaker phenotype. *FASEB J 18:1710–1712.*

Girmatsion Z., Biliczki P., Bonauer A., Wimmer-Greinecker G., Scherer M., Moritz A., Bukowska A., Goette A., Nattel S., Hohnloser S.H., Ehrlich J.R. (2009) Changes in microRNA-1 expression and IK1 up-regulation in human atrial fibrillation. *Heart Rhythm.*

Ha M. and Kim V. N. (2014) Regulation of microRNA biogenesis. *Nature Reviews molecular Cell Biology 15, 509-524.*

Heidersbach A., C. Saxby, K. Carver-Moore, Y. Huang, Y.S. Ang, P.J. de Jong, K.N. Ivey and D. Srivastava (2013) microRNA-1 regulates sarcomere formation and suppresses smooth muscle gene expression in the mammalian heart. *eLife, e01323.*

Hescheler J, Fleischmann BK, Lentini S, Maltsev VA, Rohwedel J, Wobus AM, and Addicks K (1997) Embryonic stem cells: a model to study structural and functional properties in cardiomyogenesis. *Cardiovasc Res 36:149–162.*

Hidaka K, Lee JK, Kim HS, Ihm CH, Iio A, Ogawa M, Nishikawa S, Kodama I, and Morisaki T (2003) Chamber-specific differentiation of Nkx2.5-positive cardiac precursor cells from murine embryonic stem cells. *FASEB J 17:740–742.*

Hirata H, Murakami Y, Miyamoto Y, Tosaka M, Inoue K, Nagahashi A, Jakt LM, Asahara T, Iwata H, Sawa Y, Kawamata S. (2006) ALCAM (CD166) is a surface marker for early murine cardiomyocytes. *Cells Tissues Organs. 184:172–180.*

Hoogaars WM, Tessari A, Moorman AF, de Boer PA, Hagoort J, Soufan AT, Campione M, and Christoffels VM (2004) The transcriptional repressor Tbx3 delineates the developing central conduction system of the heart. *Cardiovasc Res 62:489–499.*

Ibáñez A, Sarrias MR, Farnós M, Gimferrer I, Serra-Pagès C, Vives J, Lozano F. (2006) Mitogen-activated protein kinase pathway activation by the CD6 lymphocyte surface receptor. *J Immunol. 177(2):1152-9.*

Ivey K.N., Muth A., Arnold J., King F.W., Yeh R.F., Fish J.E., Hsiao E.C., Schwartz R.J., Conklin B.R., Bernstein H.S., Srivastava D. (2008) MicroRNA regulation of cell lineages in mouse and human embryonic stem cells. *Cell Stem Cell. 2(3):219-29.*

Jensen-Urstad K, Saltin B, Ericson M, Storck N, Jensen-Urstad M. (1997) Pronounced resting bradycardia in male elite runners is associated with high heart rate variability. *Scand J Med Sci Sports 274278.*

Kim V. N., Han J. and Siomi M. C. (2009) Biogenesis of small RNAs in animals. *Nature Rev. Mol. Cell Biol. 10, 126–139.*

Kolossov E, Lu Z, Drobinskaya I, Gassanov N, Duan Y, Sauer H, Manzke O, Bloch W, Bohlen H, Hescheler J, et al. (2005) Identification and characterization of embryonic stem cell-derived pacemaker and atrial cardiomyocytes. *FASEB J 19:577–579.*

Krol J., Loedige I. and Filipowicz W. (2010) The widespread regulation of microRNA biogenesis, function and decay. *Nature Rev. Genet. 11, 597–610.*

Lagos-Quintana M., Rauhut R., Yalcin A., Meyer J., Lendeckel W. and Tuschl T. (2002) Identification of tissue-specific microRNAs from mouse. *Curr. Biol., 12, 735–739.*

Lakatta E.G., DiFrancesco D. (2009) What keeps us ticking: a funny current, a calcium clock, or both? *Journal of Molecular and Cellular Cardiology Volume 47, Issue 2, Pages 157–170*

Lewis B.P., Burge C.B. and Bartel D.P. (2005) Conserved seed pairing, often flanked by adenosines, indicates that thousands of human genes are microRNA targets. *Cell, 120, 15-20.*

Li J., Dong X., Wang Z. and Wu J. (2014) MicroRNA-1 in Cardiac Diseases and Cancers. *Korean J Physiol Pharmacol Vol 18: 359 –363*

Li Q., Yu Q., Na R., Liu B. (2016) MiR-423-5p inhibits human cardiomyoblast proliferation and induces cell apoptosis by targeting Gab 1. *Int J Clin Exp Pathol;9(9):8953-8962*

Maltsev VA, Rohwedel J, Hescheler J, and Wobus AM (1993) Embryonic stem cells differentiate in vitro into cardiomyocytes representing sinusnodal, atrial and ventricular cell types. *Mech Dev 44:41–50.*

Maltsev VA, Wobus AM, Rohwedel J, Bader M, Hescheler J. (1994) Cardiomyocytes differentiated in vitro from embryonic stem cells developmentally express cardiac-specific genes and ionic currents. *Circ Res;75:233–244*

Mangoni M.E. and Nargeot J. (2008) Genesis and regulation of the heart automaticity. Physiol Rev.;88(3):919-82.

Maron and Pelliccia (2006) The Heart of Trained Athletes: Cardiac Remodeling and the Risks of Sports, Including Sudden Death. *Circulation. 114:1633-1644.*

Matsui Y., K. Zsebo, B.L. Hogan. (1992) Derivation of pluripotent embryonic stem cells from murine primordial germ cells in culture. *Cell 70 (4): 841-847.*

McCarthy J.J. (2011) The MyomiR network in skeletal muscle plasticity. *Exerc sport sci rev. 39(3):150-4.*

Miyamoto S., Usami S., Kuwabara Y., Horie T., Baba O., Hakuno D., Nakashima Y., Nishiga M., Izuhara M., Nakao T., Nishino T., Ide Y., Nakazeki F. (2015) expression patterns of miRNA-423-5p in the Serum and Pericardial Fluid in Patients Undergoing Cardiac Surgery; *PLOS one*

Mommersteeg MT, Domínguez JN, Wiese C, Norden J, de Gier-de Vries C, Burch JB, Kispert A, Brown NA, Moorman AF, and Christoffels VM (2010) The sinus venosus progenitors separate and diversify from the first and second heart fields early in development. *Cardiovasc Res 87:92–101.*

Mommersteeg MT, Hoogaars WM, Prall OW, de Gier-de Vries C, Wiese C, Clout DE, Papaioannou VE, Brown NA, Harvey RP, Moorman AF, et al. (2007) Molecular pathway for the localized formation of the sinoatrial node. *Circ Res 100:354–362.*

Moorman AF e Christoffels VM. (**2003)** Cardiac chamber formation: development, genes, and evolution. *Physiol Rev. 83(4):1223-67.*

Morikawa K, Bahrudin U, Miake J, Igawa O, Kurata Y, Nakayama Y, Shirayoshi Y, and Hisatome I (2010) Identification, isolation and characterization of HCN4-positive pacemaking cells derived from murine embryonic stem cells during cardiac differentiation. *Pacing Clin Electrophysiol 33:290–303.*

Morrison S. J. and Kimble J. (2006) Asymmetric and symmetric stem-cell divisions in development and cancer. *NATURE Vol 441*

Murakami Y, Hirata H, Miyamoto Y, Nagahashi A, Sawa Y, Jakt M, Asahara T, Kawamata S. (2007) Isolation of cardiac cells from E8.5 yolk sac by ALCAM (CD166) expression. *Mech Dev.124:830–839.*

Protze S., Liu J., Nussinovitch U., Ohana L., Backx P.H., Gepstein L., & Keller G.M. (2016) Sinoatrial node cardiomyocytes derived from human pluripotent cells function as a biological pacemaker. *Nature Biotechnology*

Santulli G., Iaccarino G., De Luca N., Trimarco B., and Condorelli G. (2014) Atrial fibrillation and MicroRNAs. *Front Physiol. 5: 15.*

Scavone A, Capilupo D, Mazzocchi N, Crespi A, Zoia S, Campostrini G, Bucchi A, Milanesi R, Baruscotti M, Benedetti S, et al. (2013) Embryonic stem cell-derived CD166+ precursors develop into fully functional sinoatrial-like cells. *Circ Res 113: 389–398.*

Selbach, M., Schwanhäusser, B., Thierfelder, N., Fang, Z., Khanin, R., and Rajewsky, N. (2008) Widespread changes in protein synthesis induced by microRNAs. *Nature 455: 58–63.*

Sharma S., Merghani A., and Mont L. (2015) Exercise and the heart: the good, the bad, and the ugly *European Heart Journal 36, 1445–1453*

Shi W, Wymore R, Yu H, Wu J, Wymore RT, Pan Z, Robinson RB, Dixon JE, McKinnon D, Cohen IS. **(1999)** Distribution and prevalence of hyperpolarization-activated cation channel (HCN) mRNA expression in cardiac tissues. *Circ Res. 85(1):e1-6.*

Siomi H. and Siomi M. C. (2010) Posttranscriptional regulation of microRNA biogenesis in animals. Mol. *Cell 38, 323–332.*

Smith ML, Hudson DL, Graitzer HM, Raven PB. (1989) Exercise training bradycardia: the role of autonomic balance. *Med Sci Sports Exerc 21: 404*.

St Clair JR, Sharpe EJ, Proenza C. (2015) Culture and adenoviral infection of sinoatrial node myocytes from adult mice. *Am J Physiol Heart Circ Physiol.*

Tijsen A.J., Creemers E.E., Perry D., Moerland P.D., de Windt L.J., Allard C., van der Wal A.C., Kok W.E., Pinto Y.M. (2010) MiR423-5p as a circulating biomarker for heart failure. *Circ Res. ;106(6):1035-9.*

Ulens C, Siegelbaum SA (2003) Regulation of Hyperpolarization-Activated HCN Channels by cAMP through a Gating Switch in Binding Domain Symmetry. *Neuron, Volume 40, Issue 5, Pages 959–970*

van Rooij E, Liu N, Olson EN. (2008) MicroRNAs flex their muscles. *Trends Genet. 24:159Y66.*

Viscomi C, Altomare C, Bucchi A, Camatine E, Baruscotti M, Moroni A, DiFrancesco D (2001) C Terminus-mediated Control of Voltage and cAMP Gating of Hyperpolarization-activated Cyclic Nucleotide-gated Channels. *The American Society for Biochemistry and Molecular Biology, Inc.*

Wang Z., Du W., Piazza G.A., Xi Y. (2013) MicroRNAs are involved in the self-renewal and differentiation of cancer stem cells. *Acta Pharmacologica Sinica 34: 1374–1380*

White SM and Claycomb WC (2005) Embryonic stem cells form an organized, functional cardiac conduction system in vitro. *Am J Physiol Heart Circ Physiol 288: H670–H679.*

Wiese C, Nikolova T, Zahanich I, Sulzbacher S, Fuchs J, Yamanaka S, Graf E, Ravens U, Boheler KR, and Wobus AM (2011) Differentiation induction of mouse embryonic stem cells into sinus node-like cells by suramin*. Int J Cardiol 147: 95–111.*

Wobus AM, Wallukat G, and Hescheler J (1991) Pluripotent mouse embryonic stem cells are able to differentiate into cardiomyocytes expressing chronotropic responses to adrenergic and cholinergic agents and Ca2+ channel blockers. *Differentiation 48: 173–182.*

Yang B., Lin H., Xiao J., Lu Y., Luo X., Li B., Zhang Y., Xu C., Bai Y., Wang H., Chen G. & Wng Z. (2007) The muscle-specific microRNA miR-1 regulates cardiac arrhythmogenic potential by targeting GJA1 and KCNJ2. *Nature Medicine 13, 486 – 491*

Zagotta WN, Olivier NB, Black KD, Young EC, Olson R, Gouaux (2003) Structural basis for modulation and agonist specificity of HCN pacemaker channels. *Nature;425(6954):200-5.*

Zhang H., Li W., Nan N., Ren F., Wang H., Xu Y., Zhang F. (2011) MicroRNA expression profile of colon cancer stem-like cells in HT29 adenocarcinoma cell line. *Biochemical and Biophysical Research Communications 404 273–278*

Zhao Y., Ransom J. F., Li A., Vedantham V., von Drehle M., Muth A. N., Tsuchihashi T., McManus M. T., Schwartz R. J. and Srivastava D (2007) Dysregulation of cardiogenesis, cardiac conduction, and cell cycle in micelacking miRNA-1-2. *Cell, 129, 303–317.*

Zhao H., Gao A., Zhang Z., Tian R., Luo A., Li M., Zhao D., Fu L., Fu L., Dong J., Zhu Z., (2015) Genetic analysis and preliminary function study of miR-423 in breast cancer. *Tumor Biol. 36:4763–4771*